GREEN-HOUSE GAS STORAGE THROUGH ENHANCED HYDRATE FORMATION

Thiphakorn Absuwan

A Thesis Submitted in Partial Fulfilment of the Requirements
for the Degree of Master of Science
The Petroleum and Petrochemical College, Chulalongkorn University
in Academic Partnership with
The University of Michigan, The University of Oklahoma,
Case Western Reserve University, and Institut Français du Pétrole

2018

ABSTRACT

6071016063: Petrochemical Technology Program
Thiphakorn Absuwan: Green-house Gas Storage through Enhanced Hydrate Formation.
Thesis Advisors: Prof. Pramoch Rangsunvigit and
Dr. Santi Kulprathipanja 68 pp.
Keywords: Clathrate Hydrates/ Carbon dioxide/ Tetrahydrofuran/ Sodium Dodecyl Sulfate/ Methyl Ester Sulfonate/ Hydrate Formation

The CO_2 hydrate formation in the presence of different tetrahydrofuran (THF), sodium dodecyl sulfate (SDS), and methyl ester sulfonate (MES) concentrations was investigated in terms of kinetics and thermodynamics. The formation experiment was conducted in the quiescent condition and close system at 3 MPa and 3 °C. The results showed that the CO_2 hydrates formed in the presence of 10 mol% THF, while it did not form with 5.56 mol% THF. The presence of SDS or MES did not promote the hydrate formation. However, the hydrates formed in the presence of a mixture of SDS or MES with 5.56 mol% THF. The result showed that CO_2 uptake with THF combined with SDS or MES was twice higher than that with 10 mol% THF, whereas THF combined with MES resulted in lower induction time than THF combined with SDS. Conversely, using a mixture of MES or SDS at the critical micelle concentration (CMC) and 5.56 mol% THF did not promote the hydrates formation. Surprisingly, the hydrates can form with the presence of MES or SDS at CMC and 4.5 mol% THF at the same experimental condition.

บทคัดย่อ

ทิพากร อาบสุวรรณ : การกักเก็บแก๊สเรือนกระจกผ่านกระบวนการเกิดไฮเดรต (Green-house Gas Storage through Enhanced) อ. ที่ปรึกษา : ศ.ดร. ปราโมช รังสรรค์วิจิตร และ ดร. สันติ กุลประทีปัญญา 68 หน้า

งานนี้รายงานผลศึกษาการเกิดคาร์บอนไดออกไซด์ไฮเดรตที่เติมเตตระไฮโดรฟูแรน(THF), โซเดียมโดเดซิลซัลเฟต (SDS), และเมทิลเอสเตอร์ซัลโฟเนต (MES) ที่ความเข้มข้นต่างๆ ในด้านอุณหพลศาสตร์และจลน์ศาสตร์ การศึกษาการเกิดคาร์บอนไดออกไซด์ไฮเดรตดำเนินการในสภาวะนิ่งและระบบปิดที่ความดัน 3 MPa และอุณหภูมิ 3 °C ผลการศึกษาแสดงให้เห็นว่าคาร์บอนไดออกไซด์ไฮเดรตเกิดได้ในระบบที่มี THF ความเข้มข้น 10 mol% ในขณะที่ THF ความเข้มข้น 4.5 และ 5.56 mol% ไม่สามารถทำให้เกิดไฮเดรตได้ จากผลการทดลองในระบบของ SDS และ MES พบว่าในสภาวะที่ศึกษา ไม่สามารถทำให้เกิดไฮเดรตได้ เช่นเดียวกับระบบของสารผสมระหว่างสารลดแรงตึงผิวที่ค่าความเข้มข้นวิกฤตไมเซลล์ของสารนั้นๆกับ THF ที่ความเข้มข้น 5.56 mol% อย่างไรก็ตามเมื่อลดความเข้มข้นของ THF เท่ากับ 4.5 mol% ในระบบของสารผสมกับสารลดแรงตึงผิวที่ค่าความเข้มข้นวิกฤตไมเซลล์ของสารนั้นๆ พบว่าเกิดไฮเดรตทั้งในระบบ THF ร่วมกับ SDS และ THF ร่วมกับ MES

GRAPHICAL ABSTRACT

Why do we need to capture and store CO_2?

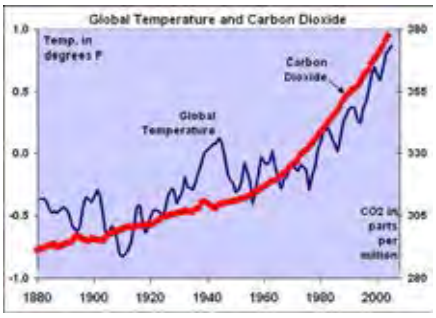

Carbon dioxide vs Global temperature graph

Source : http://zfacts.com/p/226.html

What is hydrate technology?

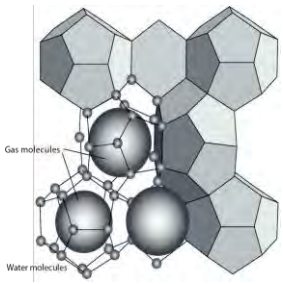

Hydrate Structure

Source: Sosso et al. (2015)

Challenges: High energy requirement

High pressure

Very low temperature

Long induction time

How to reduce energy requirement?

Promoters

Thermodynamics promoter

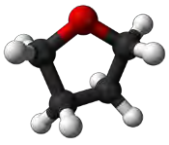

Tetrahydrofuran (THF)

- ✓ Lower pressure
- ✓ Higher temperature

Kinetics promoter

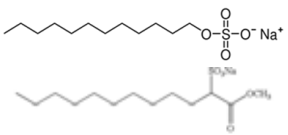

Sodium dodecyl sulfate (SDS)

Methyl ester sulfonate (MES)

- ✓ Short time
- ✓ More gas consumed

To combination 2 types of promoters.

ACKNOWLEDGEMENTS

I would like to take this chance to sincerely thanks my advisor, Prof. Pramoch Rangsunvigit, for his helpful suggestions, discussions, and supervision from very early stage of the research. He also provided me unflinching encouragement, patience and support in various ways throughout my graduate thesis.

I also would like to thanks my co-advisor, Dr. Santi Kulprathipanja, for his advice, guidance, and his willingness to share his bright thoughts with me, which was very helpful for sharing up my ideas and research.

I would like to thanks Prof. Boonyarach Kitiyanan and Dr. Tanate Danuthai for kindly serving on my thesis committee. Their suggestions are certainly important and helpful for completion of this thesis.

I would like to thanks the entire faculty and staff at The Petroleum and Petrochemical College, Chulalongkorn University for their kind assistance and cooperation.

Unfortunately, I am grateful for the scholarship and funding of the thesis provided by The 90th Anniversary of Chulalongkorn University Fund and Grant for International Integration: Chula Research Scholar, Ratchadaphiseksomphot Endowment Fund, Chulalongkorn University, Thailand; The Petroleum and Petrochemical College; and the Center of Excellence for Petrochemical and Materials Technology, Thailand.

Finally, I would like to express my sincere gratitude to thanks my whole family for showing me the joy of intellectual pursuit ever since I was a child, for standing by me and for understanding every single part of my mind.

TABLE OF CONTENTS

CHAPTER **PAGE**

CHAPTER **PAGE**

LIST OF TABLES

TABLE **PAGE**

LIST OF FIGURES

FIGURE **PAGE**

FIGURE **PAGE**

FIGURE **PAGE**

FIGURE **PAGE**

CHAPTER I
INTRODUCTION

Carbon dioxide (CO_2) as a greenhouse gas is one of major gasses contributing to the global warming. The global temperature is correlated with the CO_2 concentration. As CO_2 concentration is increased, the global temperature is also increased (Davis, 2017). Getachew and Gizaw (2018) found that current CO_2 concentration is about 403.3 ppm from 2016 and continues to increase. Although major CO_2 source is from fuel combustion process, such as coal power plant, cement industry, steel-making industry as well as petrochemical industry and so on, power generation is the largest source of CO_2 emission.

CO_2 capture technology primarily includes physical or chemical absorption, membrane technology, and cryogenic process. For the absorption, amine based absorption has been developed for a long time but it has issues with high energy for regeneration, high equipment corrosion rate, amine degradation, and solvent emission. For adsorption, solid materials with high surface area including zeolite and activated carbon are used to adsorb CO_2 gas. Limitation of this method is low CO_2 selectivity, low adsorption rate, and material degradation in cyclic operation. For membrane technology, it is still in preliminary stage of lab investigation. For cryogenic method, it can separate CO_2 with high purity. It is widely used in the commercial and suitable to separate high CO_2 concentration, typically more than 50% but the major disadvantage is that moisture must be removed from the gas mixture before cooling to prevent blockage by ice particles (Kumar *et al.*, 2012).

The fact that gas can form solid hydrates with water has been known for many years, and it has driven intensive investigations in recent years for gas separation and gas storage (Ma *et al.*, 2016). Hydrate technology has been recognized as a potential alternative for CO_2 capture. Additionally, unit per volume of gas hydrates contains hundred volumes of CO_2 gas. This technology involves no or a few chemicals and with only cold water or lean aqueous solution as a working fluid. Hydrate technology is usually carried out at high pressure and low temperature, which still poses high energy requirement. However, this technology is being developed to operate at lower energy requirement by using promoters.

Promoters can be classified into two types, kinetics and thermodynamics promoters. Thermodynamics promoters such as additives that can shift the equilibrium curve of hydrate formation for better conditions during hydrate formation (lower pressure and higher temperature than that of pure CO_2 hydrates). Kinetics promoters such as surfactants or amino acids alter the interfacial properties during gas/liquid contact resulted in the increased hydrate formation rates. These kinetics promoters have no effect on the phase equilibrium curve (Veluswamy *et al.*, 2017).

Saito (1996) investigated the possibility of storing natural gas to form hydrates by using tetrahydrofuran (THF) to get lower equilibrium pressure of the mixed hydrates. Effects of the particle size of porous media such as activated carbon, silica, and clay were also investigated. The activated carbon with 250-420 μm showed the fastest methane consumption and methane recovery, 79.2 – 99.1%, while the 841-1680 μm particle size stored the highest methane consumption and methane recovery, 75.5 – 96.5% (Siangsai *et al.*, 2015). Maize starch was reported to enhance methane hydrate formation with different concentrations. They reported that the high concentration, 800 ppm, increased the formation rate up to 2.5 times compared with no maize starch (Maghsoodloo and Abdolmohammad, 2015). Hollow silica (SiO_2) was reported to increase methane hydrate yield and rate of methane hydrate formation as well (Prasad, 2014). Seong-Pil and Jong-Won (2010) also investigated the effects of porous silica with CO_2 hydrate formation and found that porous silica enhanced hydrate formation and dissociated the induction time as well. However, the thermodynamics promoters can enhance only the equilibrium phase and the kinetics promoters can enhance only the induction of hydrate formation process. Therefore, the combination between two types of promoter may result in the synergistic effects that could improve the CO_2 hydrate formation.

In this work, THF was used as a thermodynamic promoter to form CO_2 hydrates at lower pressure and higher temperature. Sodium dodecyl sulfate (SDS) and methyl ester sulfonate (MES) were used as kinetics promoters. Moreover, this work also combined THF with MES and SDS to enhance the hydrate formation.

CHAPTER II
THEORETICAL BACKGROUND AND LITERATURE REVIEW

2.1 Carbon Dioxide Hydrates

Hydrate technology is a potential method for CO_2 capture and separation from the combustion flue gas. CO_2 hydrates can be formed under low temperature and high pressure. Hydrates are formed in solid crystalline composing of cages by water molecules like water networks as host and CO_2 molecules trapped in the cages as guest. These two molecules connect with each other by weak van der Waals force. The compound is stable when the guest is filling in the cage, otherwise, the cage becomes unstable and collapses to normal ice. There are three common forms of hydrate structure depending on the molecular diameter, structure I (sI), structure II (sII), and structure H (sH). These three structures consist of five different cages, including 5^{12}, $5^{12}6^2$, $5^{12}6^4$, $4^35^66^3$, and $5^{12}6^8$, as shown in Figure 2.1. The physical properties of these structures are different, as shown in Table 2.1(Sloan and Koh, 2007).

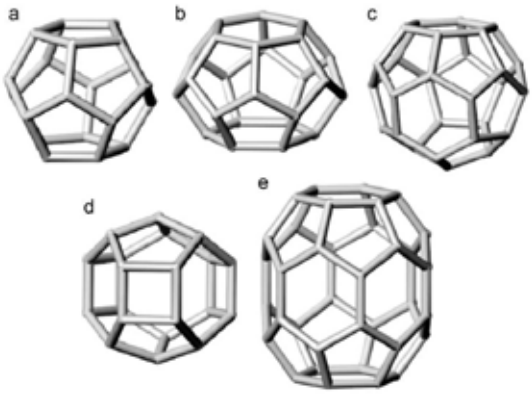

Figure 2.1 Five differences cage of gas hydrate; (a.) pentagonal (5^{12}) ; (b.) tetrakaidecahedron ($5^{12}6^2$) ; (c.) hexakaidecahedron ($5^{12}6^4$) ; (d.) irregular dodecahedron ($4^35^66^3$); and (e.) icosahedron ($5^{12}6^8$) (Sloan and Koh, 2007).

Table 2.1 Physical properties of sI, sII, and sH type gas hydrates (Sloan and Koh, 2007)

Structure	sI		sII		sH		
Cages	5^{12}	$5^{12}6^2$	5^{12}	$5^{12}6^4$	5^{12}	$4^35^66^3$	$5^{12}6^8$
Number of cages per unit cell	2	6	16	8	3	2	1
Average cage radius, 10^{-10} m	3.95	4.33	3.91	4.73	3.94	4.04	5.79
Variation in radius, %	3.4	14.4	5.5	1.73	4.0	8.5	15.1
Coordination number	20	24	20	28	20	20	36
Number of water per unit cell	46		136		34		

These three hydrate structures are composed of water molecules and five differences cage. sI consists of 46 water molecules, sII consists of 136 water molecules and sH consists of 34 water molecules, as shown in Figure 2.2 (Sun and Kang, 2016).

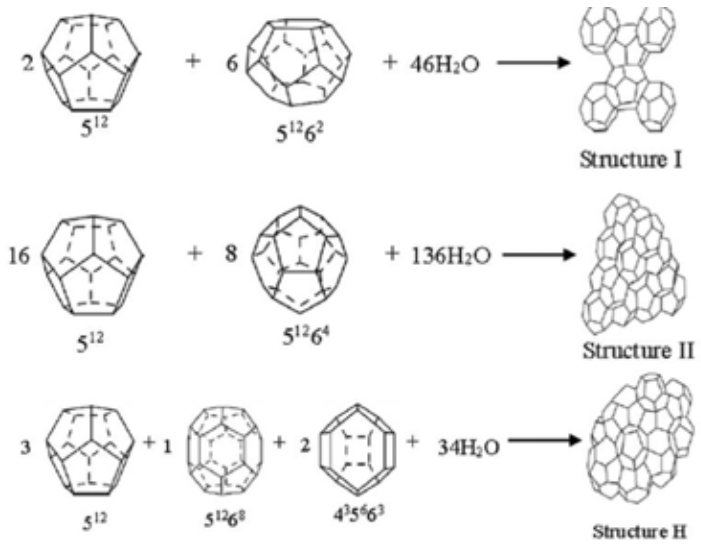

Figure 2.2 Three hydrate structure compositions (Sun and Kang, 2016).

2.2 Hydrate Formation Conditions

There are several factors that strongly influence hydrate formation, and several that have a more minor effect (neutrium.net, 2015).

Factors with strong effects on hydrate formation are:

- Dew point – the gas must be at or below the dew point for hydrates to form
- Low temperature
- High pressure
- Gas composition

Factors with more minor effects on hydrate formation are:

- Mixing
- Nucleation sites
- Kinetics
- Salinity

2.3 Hydrate Prevention and Control

The prevention of hydrate formation is preferable to remediation to ensure safety and efficiency of the plant is maintained in addition to increased difficulty and cost of remediation relative to prevention. Some common hydrate prevention techniques are described as follows (neutrium.net, 2015).

2.3.1 Temperature Control

Where suitable, a temperature control system can be implemented to keep the temperature of the gas above the dew point as hydrates will not form below this temperature. A specific dew point monitoring or moisture analyzing device can be used to aid the temperature control.

2.3.2 Water Bath Heater

A heater may be used to prevent gas from reaching the dew point. This is particularly useful when the expected temperature drop is known in advance. For example, during pressure let down through a control valve, a water bath may be used to pre-heat the gas before the valve so that the final temperature leaving the valve is above the dew point.

2.3.3 Dehydration

Reduction of the quantity of water vapor in a gas will lower the dew point and therefore lower the likelihood of hydrate formation. Several dehydration technologies are available including:

- Molecular sieves - typically a silicate compound with very small pores which can trap water molecules selectively.
- Glycol dehydration - typically triethylene glycol (TEG) although diethylene glycol (DEG), ethylene glycol (MEG) and tetraethylene glycol (TREG) may also be used.

2.3.4 Thermodynamic Inhibitors

Depression of the hydrate formation temperature can be achieved through the injection of thermodynamic inhibitors such as methanol or ethylene glycol (MEG). These inhibitors are usually required to be injected at a high rate, typically 40-60 wt% of the water content.

2.3.5 Kinetic Rate Inhibitors and Anti-agglomerates

Kinetic rate inhibitors and anti-agglomerates are usually surface-active compounds, polymers and copolymers with surfactant properties. Kinetic rate inhibitors greatly reduce the rate of formation of hydrates. Anti-agglomerates prevent the hydrates for combining together and attaching to fixed surfaces, allowing them to remain transportable through a pipeline and removed in a convenient location.

2.4 CO_2 Hydrate Formation Process

CO_2 hydrate formation includes hydrate nucleation and hydrate growth. The CO_2 consumed profile during the formation process is shown in Figure 2.3. From point A to gas dissolves in the water. From A to B, it is nucleation of hydrate, and from B to C, hydrates continue grow. Hydrate formation process is an exothermic process, while hydrate dissociation is an endothermic process (neutrium.net, 2015).

2.4.1 Hydrate Nucleation

This step is hydrate nuclei produced. Hydrate nuclei is like small labile cluster, which is made of gas and water molecules. It grows until the concentration reaches the critical point for hydrate crystal to form, as shown in Figure 2.3 (Vysniauskast and Bishnoi, 1983). Kvamme (2002) presented the theory that the hydrate nuclei initiation from the interface mainly depends on the gas transport, water surface, and adsorption characteristics. The conceptual picture is shown in Figure 2.4. The information confirmed with a report by Takeya *et al.* (2000) that the nucleation might occur on the wall near the CO_2 – water boundary.

2.4.2 Hydrate Growth

After the hydrate crystal nucleation step, the crystal growth process occurs continuously to agglomerate gas hydrates. Mass transport of gas molecules to the hydrates is important in the hydrate growth process. Moreover, the growth kinetic and heat transfer of the growth process from the crystal surface to solution are also important (Sun and Kang, 2016).

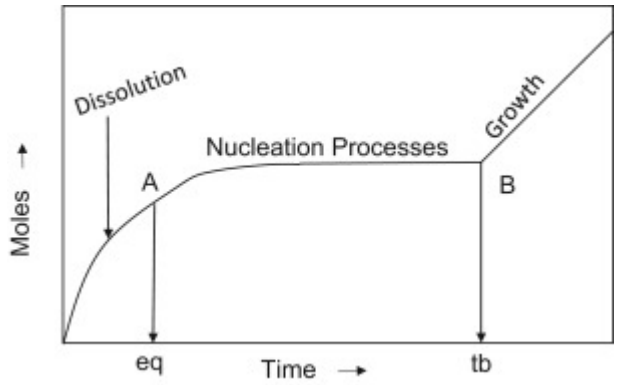

Figure 2.3 Typical gas consume during hydrate formation process (Sun and Kang, 2016).

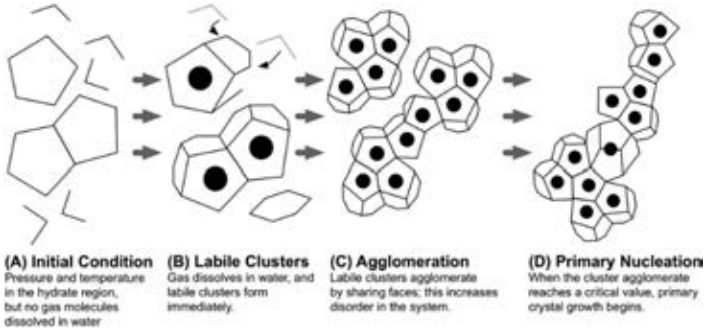

Figure 2.4 Conceptual of hydrate nucleation (Aman and Koh, 2016).

2.5 Hydrate Dissociation

Hydrate dissociation is an endothermic and vital process to eliminate hydrate crystal. The decomposition of gas hydrates to water and gas molecules can be realized by breaking hydrogen bond between water molecule and van der Waals interaction between the host and the guest molecules (Sloan and Koh, 2007). The simplified schematics of CO_2 hydrate dissociation are shown in Figure 2.5.

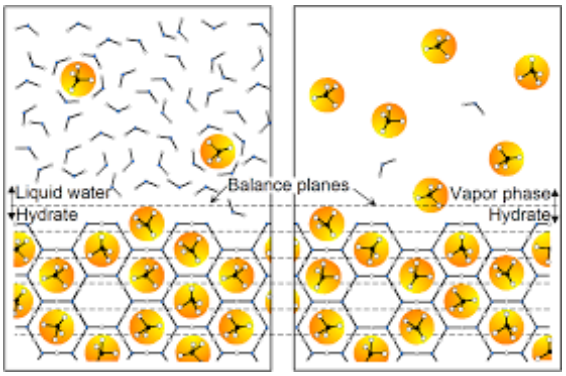

Figure 2.5 Simplified schematics of the cross section of a gas hydrate solid−fluid interface on a molecular scale. Circles: guest molecules; solid angles: water molecules; dashed lines: location of the solid−fluid interface during proposed local layer-wise decomposition. For ease of presentation, the cages are shown as hexagons (Sun and Kang, 2016).

2.5.1 Heating and Pressure Reduction

Dissociation of hydrates can be promoted through the application heat or reductions in pressure.

2.5.2 Chemical Injection

Methanol or glycol injection can be used to break down the hydrates. The conditions, under which this is appropriate strategy, depends on the positioning of the hydrates as the injected fluid must have direct contact with the hydrate formation. For example, it is unlikely to be economical to use this strategy to remove hydrates from the circumference of a long horizontal pipeline due to the requirement to fill the pipe completely.

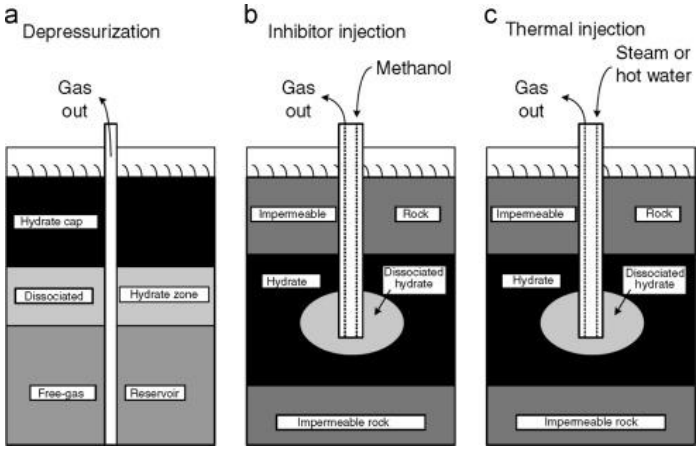

Figure 2.6 Three common ways of hydrate dissociation (Sun and Kang, 2016)

2.6 CO_2 Hydrate Promoters

2.6.1 Thermodynamic Promoters

2.6.1.1 CO_2 + tetrahydrofuran (THF) double hydrates

Tetrahydrofuran (THF) is one of the prevailing promoters for gas hydrates such as CO_2, H_2, and CH_4, or their mixtures. The equilibrium data of the tertiary system of CO_2 + THF + water is shown Figures 2.7 and 2.8, and the available property data of the corresponding hydrate are in Table 2.2.

Lirioa and Pessoab (2013) measured the equilibrium temperature of CO_2 within 5 mol% THF at 0.8 – 3.0 MPa, and dissociation heat was calculated with Clausius-Clapeyron method about 103.6 kJ/mol. The hydration number was estimated to be 13.3.

Sabil *et al.* (2010) measured the phase equilibrium of CO_2 in THF solution. Certain amount of THF was filled, and the temperature of the mixture was decreased slowly to form the hydrates. For dissociation, the heat was determined by Clausius-Clapeyron method. THF concentration was varied from 1.2 – 7 mol%, and it was found that 3 mol% THF was enough to be an effective promoter.

Table 2.2 Physical properties of CO_2 + THF hydrates

Authors	THF (mol%)	Dissociation heat (kJ/mol)	Method
Sabil *et al*. (2010)	1.2-20.6	112.4-152.3	Clausius-Clapeyron 10-14°C
Lirioa and Pessoab (2013)	5	130.6	Clausius-Clapeyron 10-19°C, 0.8-3.0 MPa
Anthony *et al*. (2006)	3.8-15	130-163	Modeling and calorimetry Clausius-Clapeyron 6.85°C, 0.2-3.5 MPa

Moreover, they also explored the additives like NaCl, KCl, and NaB in THF solution to promote the CO_2 hydration formation. It was reported that the metal halides can reduced the THF promotion.

Anthony *et al.* (2006) identified the CO_2 hydrates in THF aqueous condition by differential thermal analysis (DTA) and differential scanning calorimetry (DSC). They also developed the model of hydrate formation by combining van der Waals and Platteeuw model and predicted phase equilibrium temperature. Dissociation heat of the CO_2 + THF double hydrates was calculated by Clasius-Clapeyron method. The heat is increased from 130 kJ/mol to 163 kJ/mol with increasing THF concentration from 3.8 wt% to 15 wt%. They concluded that the enthalpy increase was due to the change of hydrate structure from sI to sII when THF involved in CO_2 hydrates.

Veluswamy *et al.* (2017) presented the phase equilibrium of CO_2 + water hydrate and CO_2 + THF as shown in Figure 2.8. They also studied effect of THF and SDS on CO_2 hydrate growth at 5.6 mol%THF, 3.0 MPa, and 283.2 K with visual observations during the hydrate formation for the first 60 min from nucleation. As seen from Figure 2.9, only limited hydrate formation was observed, and the total CO_2 uptake recorded for this experiment was only 2.9 mmol of gas/mol of water after

2 hours from nucleation. The visual observations for the same time showed that the gas uptake for THF/CO_2 system was about 20 times lower than CH_4 uptake. This behavior is also in sharp contrast to the solubility of guest gases studied CO_2, which has higher solubility in THF solution than CH_4 (CO_2 solubility in water is approximately 80 times higher than that of methane). THF promoter was shown to demonstrate a synergistic behavior enhancing hydrate formation in the presence of methane in unstirred configuration compared to highly soluble CO_2 guest gas under studied experimental conditions. Another plausible reason could be that the smaller methane molecule (diameter 4.36 A) can readily occupy the small cages of sII structure unlike CO_2 (having slightly larger diameter 5.12 A) hence resulting in decreased gas uptake despite the higher solubility (Veluswamy *et al.*, 2017).

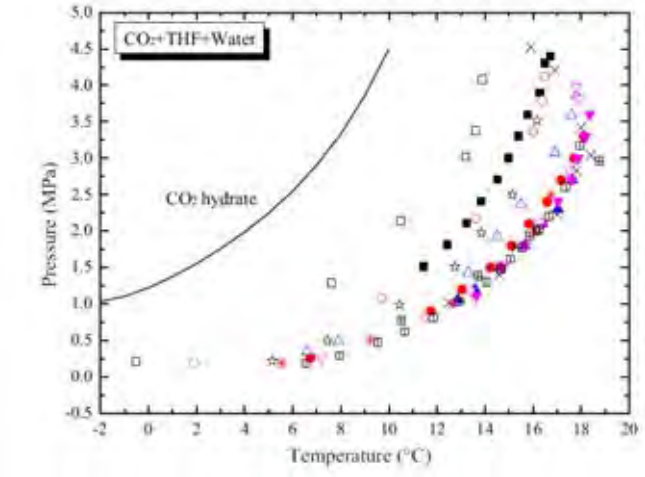

Figure 2.7 Phase equilibrium data of CO_2 + THF + water system; Sabil et al., ■ 1 mol%, 3 mol%, ▲ 5 mol%, ▼ 7 mol%; Lirio et al., ⊞ 5 mol%; Delahaye et al., ☆ 1.56mol%, ✳ 2.75 mol%; Seo et al., □ 1 mol%, ○ 2 mol%, △ 3 mol%, ▽ 5 mol%; Yang et al., 3 mol%; And Lee et al., ◫ 5.56 mol% Percentages are the used THF solution concentrations (Ma *et al.*, 2016).

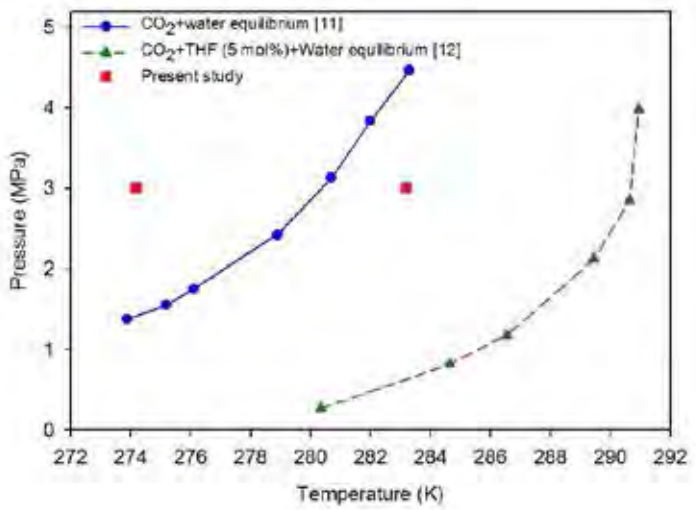

Figure 2.8 Phase equilibrium plots for CO_2+water system and CO_2+THF+water system (Veluswamy *et al.*, 2017).

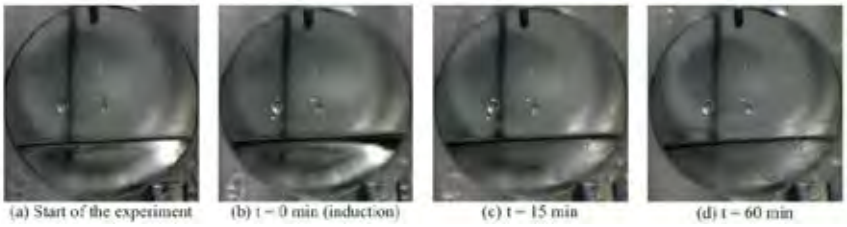

Figure 2.9 Visual observations of mixed CO_2/THF hydrates under similar experimental conditions (Veluswamy *et al.*, 2017).

2.6.1.2 CO_2 + tetra-n-butyl ammonium bromide (TBAB) double hydrates

Tetra-n-butyl ammonium bromide (TBAB) is a promoter that is widely popular for CO_2 hydration. The phase equilibrium of CO_2 + TBAB + water system was measured by many researchers as shown in Table 2.3.

Table 2.3 Thermo – physical properties of hydrate of CO_2 + TBAB

Authors	TBAB (wt%)	Dissociation heat (kJ/mol CO_2)	Method
Lin *et al*. (2008)	4.43	168.2	Clausius–Clapeyron
		9.65 °C	
	9.01	139.5	Calorimetry
		203.6	Clausius–Clapeyron
Johnny and Didier (2009)	40	346–395.8	Calorimetry
		13.35–15.45 °C	

Lin *et al.* (2008) determined the phase equilibrium of CO_2 hydrates with 4.43, 7.02 and 9.01wt% TBAB solution with a differential thermal analysis (DTA) device. Both calorimetry and Clausius–Clapeyron methods were used to acquire the dissociation heat of hydrate, and the results were 139.5kJ/mol (CO_2) and 203.6 kJ/mol (CO_2), respectively.

Johnny and Didier (2009) measured the dissociation heat of CO_2 + TBAB hydrate with 40 wt% TBAB solution, which was 346.0 – 395.8 kJ/kg water by DSC method.

2.6.2 Kinetic Promoters

2.6.2.1 CO_2 + sodium dodecyl sulfate (SDS) hydrates

Kinetic promoters like surfactants alter the gas/liquid interfacial properties due to which increased hydrate formation rates are achieved. These kinetic promoters have no effect on the phase equilibrium curve, thus the addition of kinetic promoters does not result in any change in operating conditions of hydrate formation and hydrate phase equilibrium.

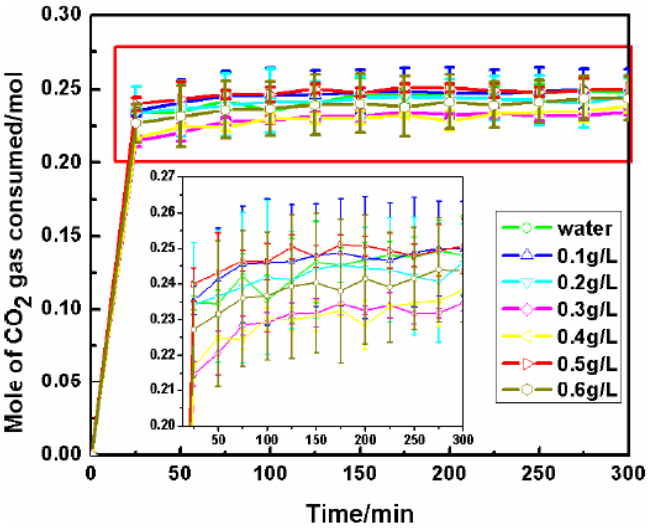

Figure 2.10 CO_2 consumption on hydrate formation for different SDS concentrations at 274.15 K and 5 MPa (Lele *et al.*, 2016).

Lele *et al.* (2016) applied seven different concentrations of SDS to CO_2 hydrate formation. Results are in Figure 2.10. As seen from the figure, the CO_2 consumption increased with the presence of SDS in all studied concentrations compared to that without agitating or no surfactants. The maximum amount of CO_2 gas consumption was 0.251 moles with SDS. The storage capacity of CO_2 hydrates, volume of CO_2 release per unit volume of hydrates at standard condition, in SDS solution at 274.15 K and 5.0 MPa within 300 min was calculated and shown in Figure 2.11.

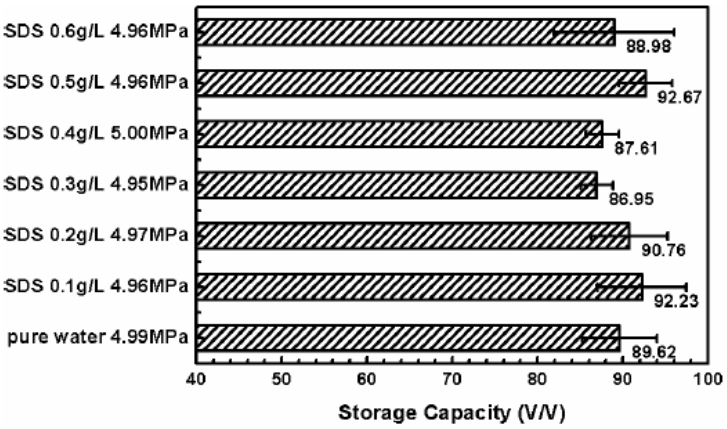

Figure 2.11 Storage capacity of CO_2 hydrate for each concentration of SDS at 274.15 K and 5.0 MPa within 300 minutes (Lele *et al.*, 2016).

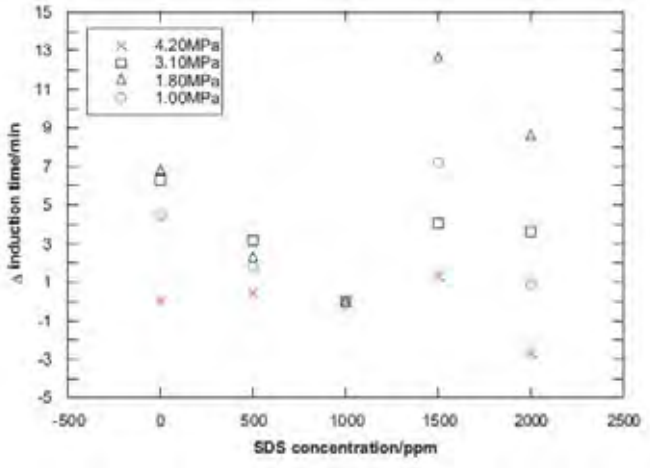

Figure 2.12 Induction time relative to that of 1,000 mg/L SDS (Yang *et al.*, 2013).

Yang *et al.* (2013) reported the induction time with different conditions for CO_2 hydrate formation by using SDS, as shown in Figure 2.12. The time differences were calculated by

$$\Delta t = t_{i,j} - t_{i,3.1} \qquad (2.1)$$

where t = time required for hydrate formation

i = concentration of SDS (0, 500, 1000, 1500, 2000 mg/L)

j = pressure (4.20, 3.10, 1.80, 1.00 MPa)

At 4.20 MPa, the time difference was smaller than the other pressure conditions and had only negative value, which means that the formation time at 2,000 mg/L SDS was the shortest. However, the difference was small at the low SDS concentrations. The induction time differences approached one another at the low pressures and low SDS concentrations. The largest difference was for 1,500 mg/L and 1.80 MPa. When the SDS concentration reached 2,000 mg/L, the order of the time difference was 1.80 MPa, 3.10 MPa, and 1.00 MPa (Yang *et al.*, 2013).

Figure 2.13 Visual observations of mixed CO_2/SDS hydrates under similar experimental conditions (Veluswamy *et al.*, 2017).

Veluswamy *et al.* (2017) performed CO_2 + 0.05 wt% SDS hydrate formation at 3.0 MPa and 274.2 K (in the absence of THF promoter). The 0.05 wt% SDS was the optimal concentration reported. The mechanism of hydrate growth presented in Figure 2.13 (v-z). They observed that SDS improved the formation kinetics with hydrate growth above the gas/liquid interface and gas uptake of about 16.9 mmol gas/mole of water at the end of two hours.

2.6.2.2 CO_2 + silica gel hydrates

Seo and Kang (2010) reported that the gas hydrate formation rate can be faster in porous silica gel than the bulk phase. The hydrates can be formed faster in the porous silica gels (Seong-Pil and Jong-Won, 2010). They concluded that porous media provided the contacts area for gas molecules and water molecules in the pores.

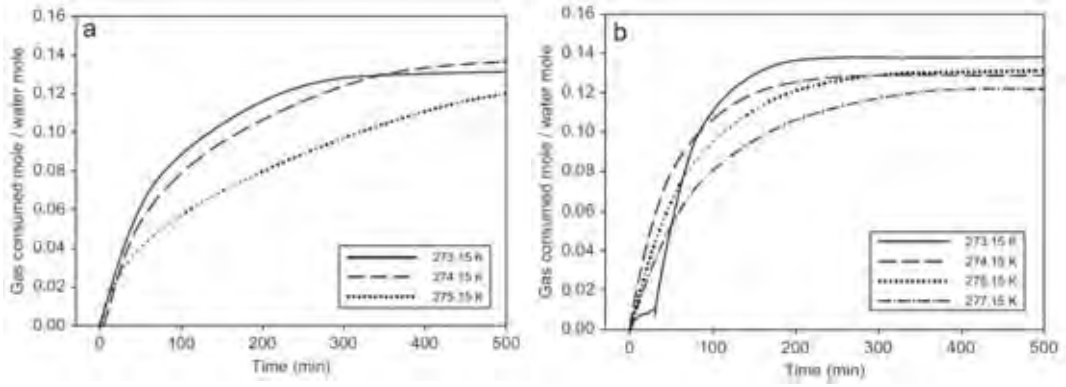

Figure 2.14 Kinetics of CO_2 + water hydrate formation in silica gels at various temperatures (a) formation pressure of 2.0 MPa; (b) formation pressure of 3.0 MPa (Seong-Pil and Jong-Won, 2010).

Seong-Pil and Jong-Won (2010) studied CO_2 hydrate formation behavior at various temperatures and a given pressure, as shown in Figure 2.14. At 2.00 MPa, the initial formation rate was difference at various temperatures. At 3.00 MPa, increasing the driving force affected the initial formation rate. For a temperature of 273.2 K, the final consumption value is the highest but the induction time was delayed. For the other temperatures that the initial formation rate affects time taken to store desired amount of gas.

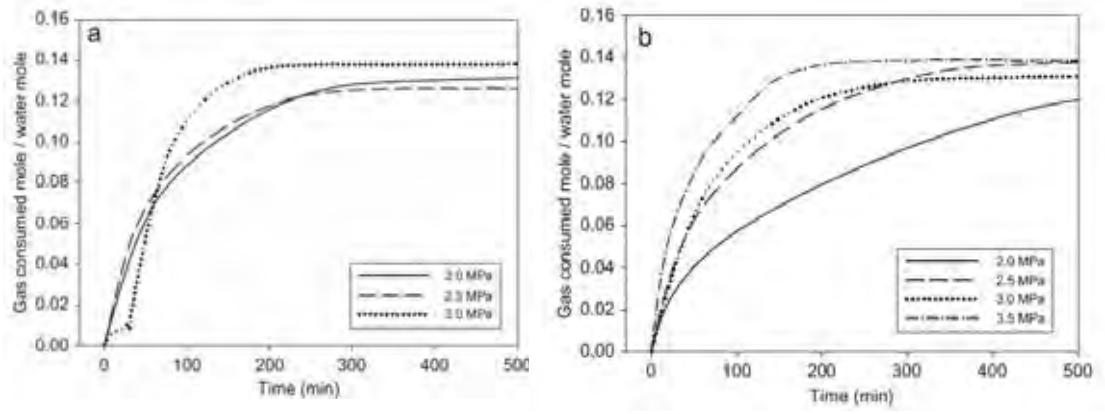

Figure 2.15 Kinetics of CO_2 + water hydrate formation in silica gels at various pressures (a) formation temperature of 273.2K; (b) formation temperature of 275.2 K (Seong-Pil and Jong-Won, 2010).

Figure 2.15 shows the formation kinetics of CO_2 hydrates with 100 nm porous silica gels at various pressures and temperature. For 273.2K and 275.2K, the final CO_2 gas consumption increased with increase in the formation pressure. Moreover, it can be concluded that the hydrate formation rate mainly depended on the driving force. For both temperatures, CO_2 hydrates were found to form faster as the driving force increased (Seong-Pil and Jong-Won, 2010).

2.6.2.3 CO_2 + sodium dodecyl sulfate (SDS) + silica gel hydrates

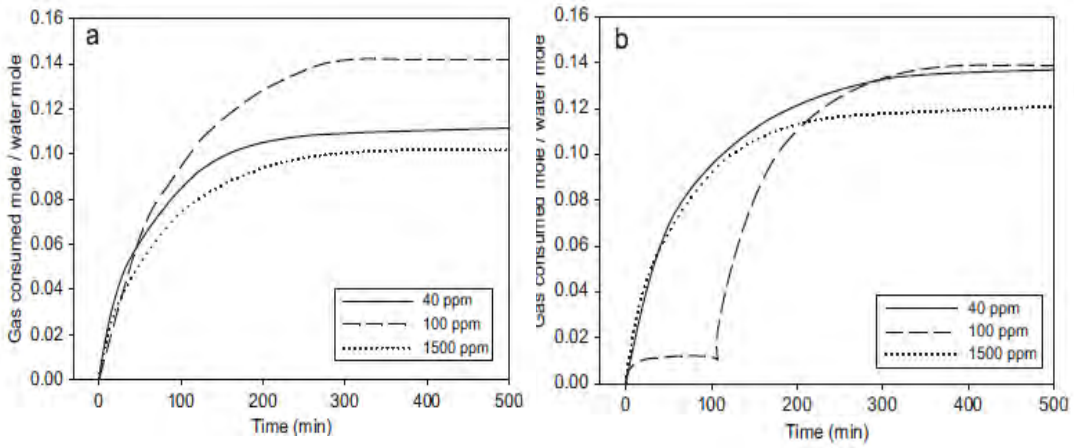

Figure 2.16 Effects of a kinetic promoter (SDS) at various concentrations on the formation behaviors of binary CO_2 + water in silica gels: (a) formation conditions of 273.2 K and 2.0 MPa; (b) formation conditions of 275.2 K and 3.0 MPa (Seong-Pil and Jong-Won, 2010).

Figure 2.16 shows formation rates and final gas consumptions when 40, 100 and 1500 ppm of the promoters were used. The final gas consumption usually increased as the promoter concentration or driving force increased. However, it should be noted that the promoter concentration of 100 ppm showed the highest gas consumption for both cases. Seong-Pil and Jong-Won (2010) inferred that the promoter concentration might have an optimum value, and the concentration higher than the optimum can act as an inhibitor for hydrate formation. Some publications also argued that a characteristic of hydrate formation was the solubility of a promoter, not the critical micelle concentration (CMC) (Kazunori *et al.*, 2008) (Watanabe *et al.*, 2005). As pointed out by Watanabe *et al.* (2005), the addition

of SDS up to the CMC significantly increased the hydrate formation rates, while further increase in the SDS concentration slightly inhibited the formation rates.

CHAPTER III
EXPERIMENTAL

3.1 Materials and Equipment

3.1.1 Chemicals

1. Tetrahydrofuran (THF)
2. Methyl Ester Sulfonate (MES)
3. Sodium Dodecyl Sulfate (SDS)
4. Deionized water

3.1.2 Equipment

Hydrate formation and dissociation apparatus

1. Crystallizer (CR)
2. Reservoir (R)
3. Personal Computer (PC)
4. Pressure transducer (PT)
5. K-type thermocouple
6. Controllable water bath

3.2 Experimental Procedures

3.2.1 Experimental Apparatus

Figure 3.1a shows the schematic and cross section of gas hydrate apparatus. The main tools of this system consisted of a high-pressure stainless-steel crystallizer (CR), a reservoir (R), and a crystallizer. The reservoir was immersed in a cooling bath, the temperature of which was adjusted and controlled by an external controllable circulator. The pressure transducers were used to measure the pressure. The temperature in the crystallizer was measured by using k-type thermocouples. Figure 3.1b shows the cross section of crystallizer and the locations where the thermocouples were located: T1 at the top of the bed, T2 at the middle of the bed, T3 at the bottom of the bed, and T4 at the bottom of the crystallizer. The data of

experiments was collected through a computer to chronicle pressure and temperature during the experiment by using A data logger (AI210 Model, Wisco Industrial instruments, Thailand). All experiments were carried out in the quiescent condition with a fixed amount gas and water in the closed system.

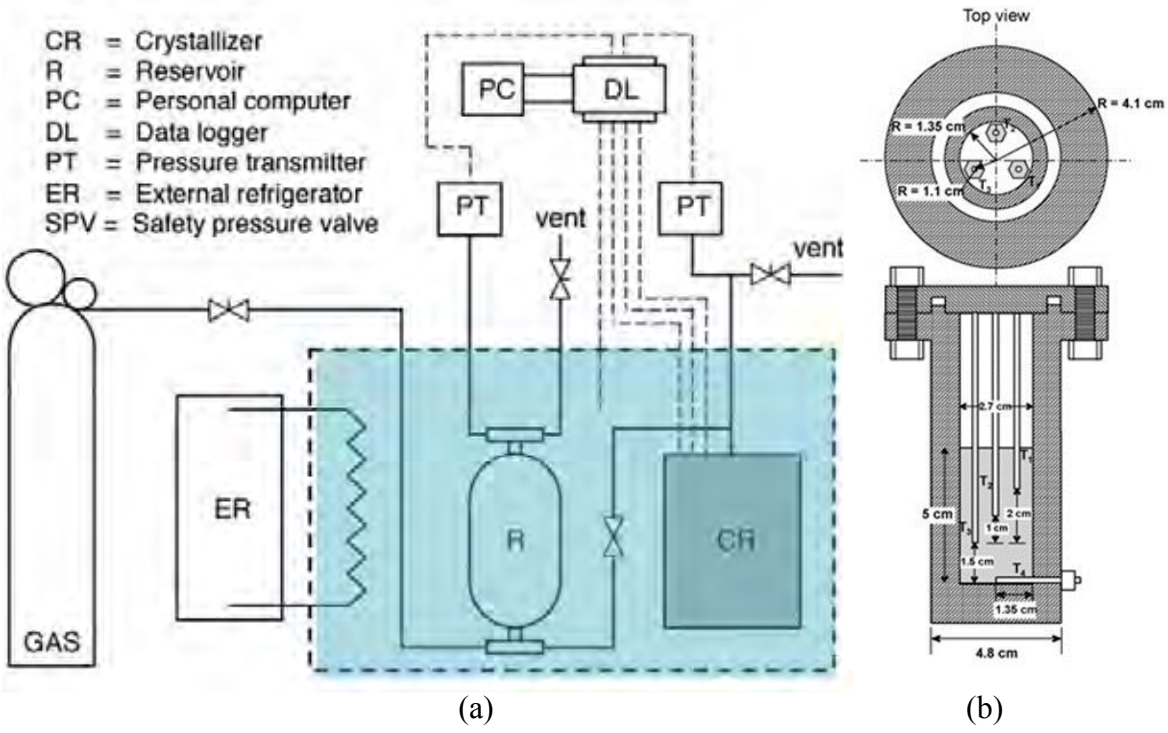

Figure 3.1 Schematic diagram of gas hydrate apparatus; a) schematic diagram, b) cross-section of a crystallizer (Siangsai *et al.*, 2015).

3.2.2 Carbon Dioxide Hydrate Formation

The experimental apparatus was cleaned by using deionized water and purged with carbon dioxide to ensure that the reactor was thoroughly clean.

↓

Evacuated until the reactor was cooled and the temperature was stabilized.

↓

Carbon dioxide gas was introduced into the system rapidly until the system pressure reached the desired experimental pressure (3 and 4 MPa), and the data was recorded every 10 sec.

↓

All experiments were carried out in the fixed condition of water and gas in the system. The experiments continued until no significant change in the pressure.

↓

The pressure and temperature data were used to calculate for the carbon dioxide consumption (gas uptake) using following Equation (3.1) (Babu *et al*., 2013).

$$\Delta n_{H\downarrow} = n_{H,t} - n_{H,0} = \left(\frac{PV}{zRT}\right)_{G,0} - \left(\frac{PV}{zRT}\right)_{G,t} \quad (3.1)$$

where $\Delta n_{H\downarrow}$ = moles of consumed gas for hydrate formation (mole)

$n_{H,t}$ = moles of hydrate at time t, (mole)

$n_{H,0}$ = moles of hydrate at time 0, (mole)

P = pressure of the crystallizer, (atm)

T = temperature of the crystallizer, (K)

V = the volume of gas phase in the crystallizer, (cm^3)

z = compressibility factor

R = the universal gas constant 82.06 cm^3.atm/mol.K

Subscripts of G, 0 and G, t are the gas phase at time zero and time t respectively. The conversion of water to hydrate was calculated by Equation (3.2) (Babu *et al*., 2013).

$$\text{Conversion of water to hydrates} = \frac{\Delta n_{H\downarrow} \text{ x hydration number}}{\Delta n_{H_2O}} \text{ x } 100 \quad (3.2)$$

where Δn_{H_2O} = moles of water in the system, mole

$\Delta n_{H\downarrow}$ = moles of consumed gas for hydrate formation, mole

Hydration number is the number of water molecules per gas molecules.

3.2.3 Carbon Dioxide Hydrate Dissociation

After carbon dioxide hydrate formation, the hydrates were dissociated by using thermal stimulation.

The temperature was increased from the formation temperature to desired dissociation temperature by setting the desired temperature at the cooler.

↓

Carbon dioxide gas was released until the system pressure reached the desired experimental temperature and the data will be recorded in every 10 sec.

The desired temperature point was marked as time zero for the hydrate dissociation experiments. The total moles of gas in the system equal to the moles of gas at time zero. At any given time, the total number of moles ($n_{H,t}$) in the system remains constant and equals to that at time zero ($n_{H,o}$). Therefore, the mole of released carbon dioxide from the hydrate at any time during the hydrate dissociation was calculated by Equation (3.3) (Siangsai *et al.*, 2015).

$$\Delta n_{H\uparrow} = n_{H,0} - n_{H,t} = \left(\frac{PV}{zRT}\right)_{G,t} - \left(\frac{PV}{zRT}\right)_{G,0} \qquad (3.3)$$

where $\Delta n_{H\uparrow}$ = moles of consumed gas for hydrate dissociation (mole)

$n_{H,t}$ = moles of hydrate at time t, (mole)

$n_{H,0}$ = moles of hydrate at time 0, (mole)

P = pressure of the crystallizer, (atm)

T = temperature of the crystallizer, (K)

V = the volume of gas phase in the crystallizer, (cm3)

z = compressibility factor

R = the universal gas constant 82.06 cm^3.atm/mol.K

Subscripts of G, 0 and G, t represent the gas phase at time zero and time t respectively. The methane recovery was calculated by Equation (3.4) as a function of time for any dissociation experiment based on its information of formation experiment (Siangsai *et al.*, 2015).

$$\% \text{ carbon dioxide recovery} = \frac{\Delta n_{H\uparrow}}{\Delta n_{H\downarrow}} \times 100 \qquad (3.4)$$

where $\Delta n_{H\uparrow}$ = moles of consumed gas for hydrate dissociation, (mole)

$\Delta n_{H\downarrow}$ = moles of consumed gas for hydrate formation, (mole)

CHAPTER IV
RESULTS AND DISCUSSION

In this study, CO_2 hydrate formation with thermodynamics and kinetics promoter was carried out. Tetrahydofuran (THF) was used as thermodynamics promoter, while sodium dodecyl sulfate (SDS), and methyl ester sulfonate (MES) were used as kinetics promoters. The gas consumed, released, and recovery calculation are show in the appendix.

4.1 Effects of Single Promoters

4.1.1 Effects of Tetrahydrofuran (THF)

4.1.1.1 CO_2 Hydrate Formation

CO_2 consumed from hydrate formation with THF at 3 °C and 3 MPa are in Table 4.1. CO_2 hydrates form in the presence of 10.00 mol% THF, while it is not the case for 4.5 and 5.56 mol% THF. The CO_2 consumed in the system of 10.00 mol% THF at 3 °C and 3 MPa is 33.53 ± 6.94 mmol/mol water, and the induction time is lower than 5 min. However, in the presence of 4.50 and 5.56 mol% THF, although there is no hydrate formation, CO_2 is consumed, 7.53 ± 5.140 and 7.69 ± 0. 31 mmol/mol.

Figure 4.1 shows CO_2 hydrate formation experiment in the presence of 4.5 mol% THF at 3 °C and 3 MPa. The temperature profiles are relatively constant for 13 hours referring to no hydrate formation. In the case of 5.56 mol% THF, the temperature profiles during the hydrate formation are also relatively constant, as shown in Figure 4.2. However, with the presence of 10.00 mol% THF, there is an evidence of hydrate formation as indicated by the temperature spikes, Figure 4.3. As seen in the figure, the amount of gas uptake increases because of dissolution CO_2 into water until it saturates. Then, the rate of gas uptake suddenly increases due to the formation of CO_2 hydrates in the system (Sun and Kang, 2016). The temperature of all thermocouples rise at the same time showing the hydrate formation in different

locations at about the same time. Hydrates continue to grow until the gas uptake reaches the plateau at 240 min.

Table 4.1 CO_2 hydrate formation experiments with the presence of 4.50, 5.56, and 10.00 mol% THF

Exp.	Promoter compositions	[a]Induction time (min)	CO_2 consumed (mmol/mol of water)
	Water	[b]	-
1	4.50 mol% THF	[b]	3.89
2	4.50 mol% THF	[b]	11.16
		Average	7.53 ± 5.14
3	5.56 mol% THF	[b]	7.87
4	5.56 mol% THF	[b]	7.51
		Average	7.69 ± 0. 31
5	10.00 mol% THF	1	25.72
6	10.00 mol% THF	5.67	28.62
		Average	27.17 ± 2.05

[a]Induction Time = time at the first hydrate formation

[b]No CO_2 hydrates formed during 13 hours of the experiment

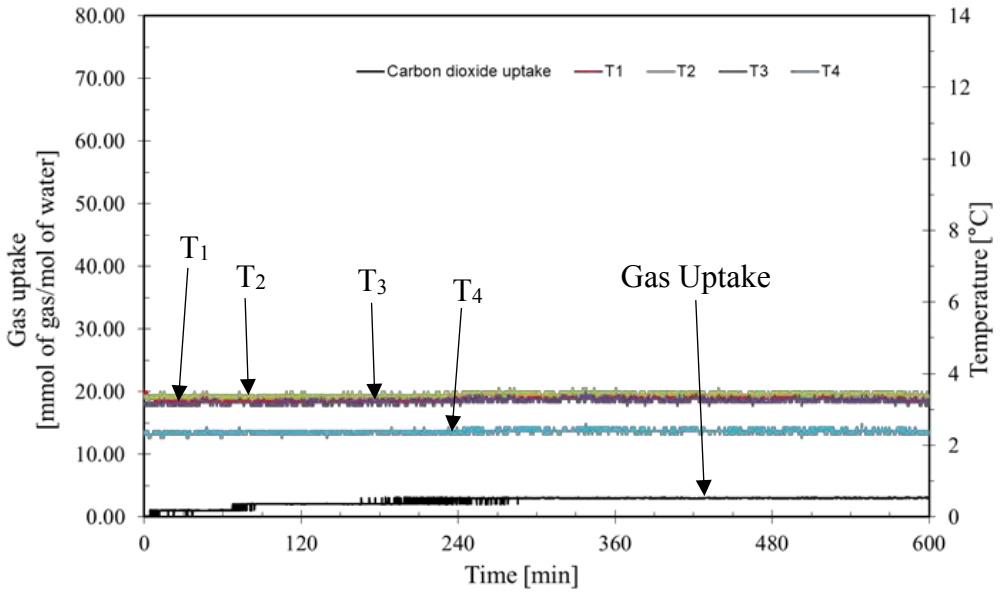

Figure 4.1 CO_2 hydrate formation experiment at 3 °C and 3 MPa in the presence of 4.5 mol% THF (Experiment No.1).

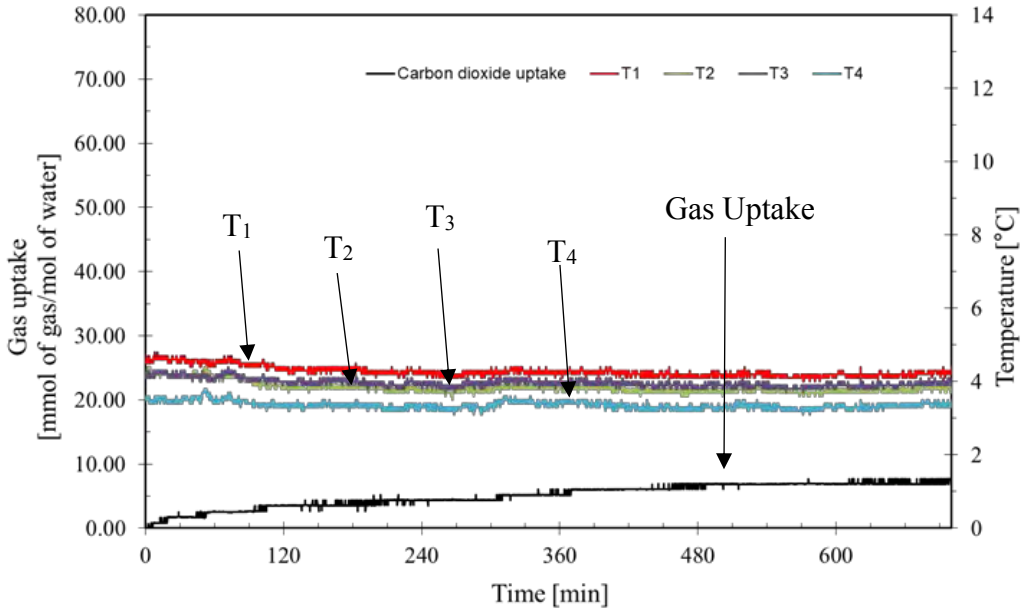

Figure 4.2 CO_2 hydrate formation experiment at 3 °C and 3 MPa in the presence of 5.56 mol% THF (Experiment No.3).

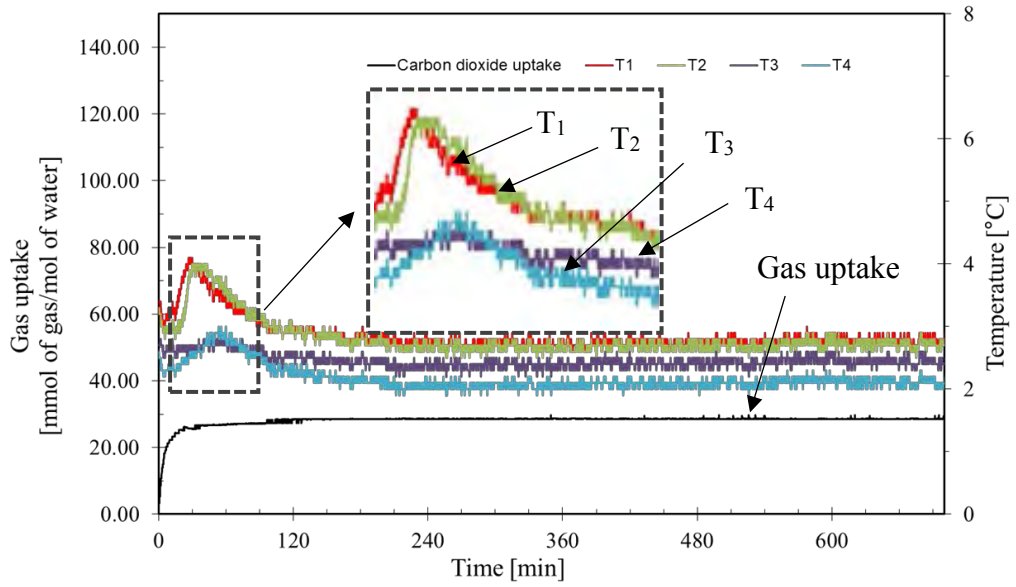

Figure 4.3 CO_2 hydrate formation experiment at 3 °C and 3 MPa in the presence of 10.00 mol% THF (Experiment No.6).

4.1.1.2 CO_2 Hydrate Dissociation

The dissociation experiment starts after hydrate formation were completed. Thermal stimulation method was used to dissociate CO_2 hydrates by setting the temperature to 35 °C. Figure 4.4 shows the dissociation of CO_2 hydrates formed in the presence of 10.00 mol% THF. When the temperature crosses the hydrate boundary, the hydrates dissociate and CO_2 gas releases. The experiment is stopped when the temperature and pressure is constant. The hydrate dissociation is an endothermic reaction. Therefore, the decrease in the temperature in the crystallizer can be observed. Table 4.2 shows the average percentage of CO_2 recovery at the end of the experiment. It can be observed that some CO_2 still remains in the solution that cannot be recovered.

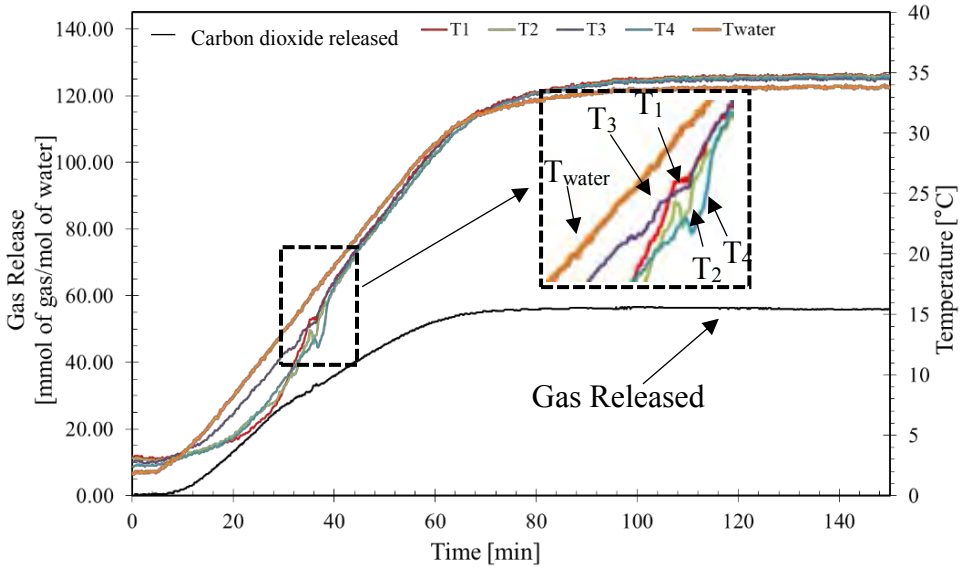

Figure 4.4 Dissociation of CO_2 hydrates formed in the presence of 10.00 mol% THF (Experiment No.5).

Table 4.2 CO_2 hydrate dissociation experiments for the hydrates formed with 10.00 mol% THF at 35 °C

Exp.	**Promoter compositions**	**CO_2 released (mmol/mol of water)**	**CO_2 recovery (mol%)**
5	10.00 mol% THF	42.86	54.35
6	10.00 mol% THF	5.76	18.05
	Average	24.31 ± 26.23	36.20 ± 25.67

4.1.2 CO_2 Hydrate Formation with Methyl Ester Sulfonate (MES)

The gas uptake and temperature profiles during the CO_2 hydrate formation experiments in the presence of 2 and 4 mM MES is shown in Figures 4.5 and 4.6, respectively. The temperature profiles are relatively constant for 13 hours. However, CO_2 dissolution into the solution can be observed. That is likely because the interfacial tension between gas and water is decreased from the presence of MES. Therefore, the solubility of CO_2 in the solution is increased and the inter phase diffusion resistance is decreased. Note that the critical micelle concentration (CMC) of MES in water is 4 mM (Roberts *et al.*, 2008). Moreover, the CO_2 consumption in the system with MES is higher than that with 4.5 and 5.56 mol% THF. As shown in Table 4.3, CO_2 hydrates do not form with the presence of 2 and 4 mM MES at 3 °C and 3 MPa.

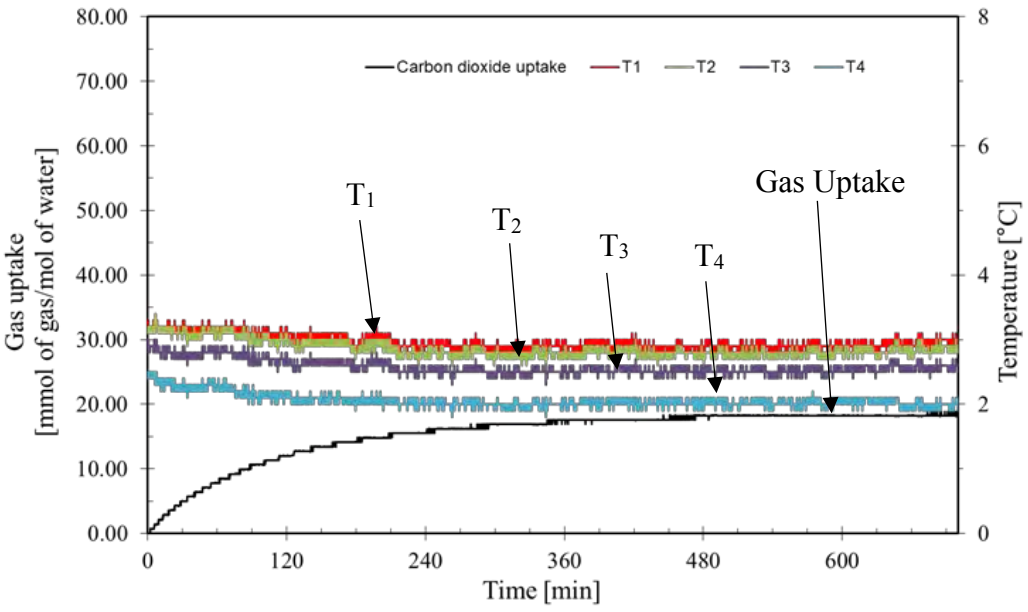

Figure 4.5 CO_2 hydrate formation experiment at 3 °C and 3 MPa in the presence of 2 mM of MES (Experiment No.7).

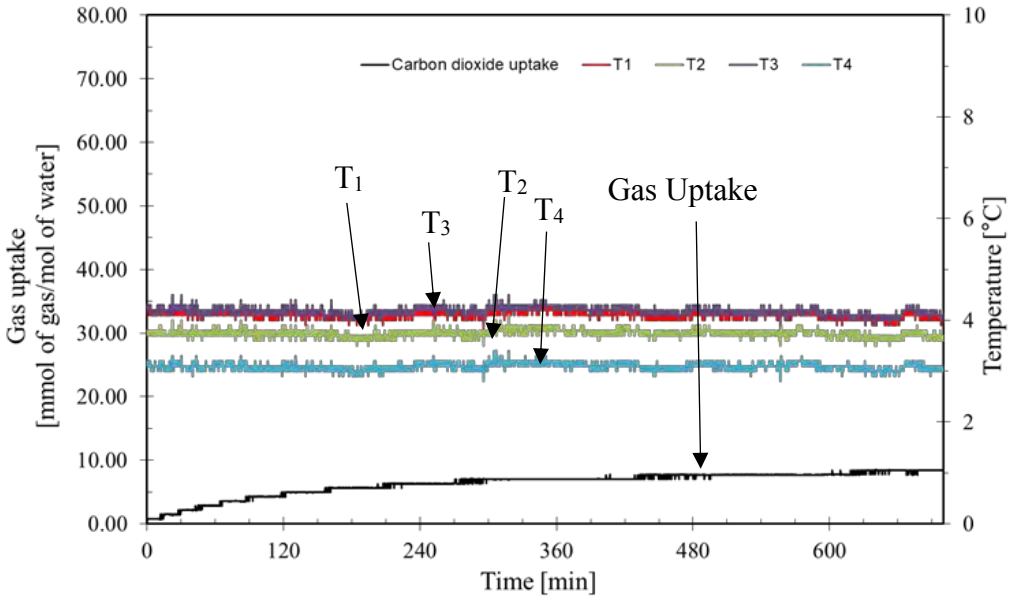

Figure 4.6 CO_2 hydrate formation experiment at 3 °C and 3 MPa in the presence of 4 mM of MES (Experiment No.9).

Table 4.3 CO_2 hydrate formation experiments with the presence of 2 and 4 mM MES

Exp.	Promoter compositions	[a]Induction time (min)	CO_2 consumed (mmol/mol of water)
	Water	[b]	-
7	2 mM MES	[b]	22.44
8	2 mM MES	[b]	18.81
		Average	20.63 ± 2.57
9	4 mM MES	[b]	8.40
10	4 mM MES	[b]	6.35
11	4 mM MES	[b]	26.28
		Average	13.67 ± 10.96

[a]Induction Time = time at the first hydrate formation

[b]No CO_2 hydrates formed during 13 hours of the experiment

4.1.3 CO_2 Hydrate Formation with Sodium Dodecyl Sulfate (SDS)

Effects of SDS on CO_2 hydrate formation were investigated with the presence of 2.28, 4, and 8.2 mM SDS at 3 °C and 3 MPa. The results are shown in Table 4.4. Although Aman and Koh (2016) reported that 650 ppm or 2.28 mM SDS into water resulted in the highest methane uptake at 3 °C and 6.6 MPa in a stirred system. In this work, the addition of 2.28 mM SDS does not enhance the CO_2 hydrate formation. The CMC of SDS, 8.2 mM, does not promote CO_2 hydrate formation in the quiescent system. The same results are observed with the addition of 4 mM SDS. It should be pointed out that, despite of the lowest surface tension of the solution with the highest dissolution of CO_2, there is no CO_2 hydrates formed (Roosta *et al.*, 2014, Veluswamy *et al.*, 2017).

The gas uptake and temperature profiles during the experiments in the presence of 2.28, 4, and 8.2 mM SDS are shown in Figures 4.7 – 4.9, respectively. The CO_2 consumed in the presence of SDS is higher than THF because SDS is a surfactant that can reduce the surface tension between the gas and liquid phases. Moreover, CO_2 consumed in the presence of SDS is slightly more than the MES. That is probably due to the SDS structure that has more hydrocarbon atoms than MES resulting in more hydrophobicity. The higher of hydrophobicity as same as CO_2 because it is rather a nonpolar molecule that has a linear and symmetrical structure, with two oxygen atoms of equal electronegativity pulling the electron density from carbon.

Table 4.4 CO_2 hydrate formation experiments with the presence of 2.28, 4, and 8.2 mM SDS

Exp.	Promoter compositions	[a]Induction time (min)	CO_2 consumed (mmol/mol of water)
	Water	[b]	-
12	2.28 mM SDS	[b]	29.50
13	2.28 mM SDS	[b]	21.95
		Average	25.73 ± 5.34
14	4 mM SDS	[b]	27.71
15	4 mM SDS	[b]	25.71
		Average	26.71 ± 1.41
16	8.2 mM SDS	[b]	13.42
17	8.2 mM SDS	[b]	17.43
		Average	15.425 ± 2.84

[a]Induction Time = time at the first hydrate formation

[b]No CO_2 hydrates formed during 13 hours of the experiment

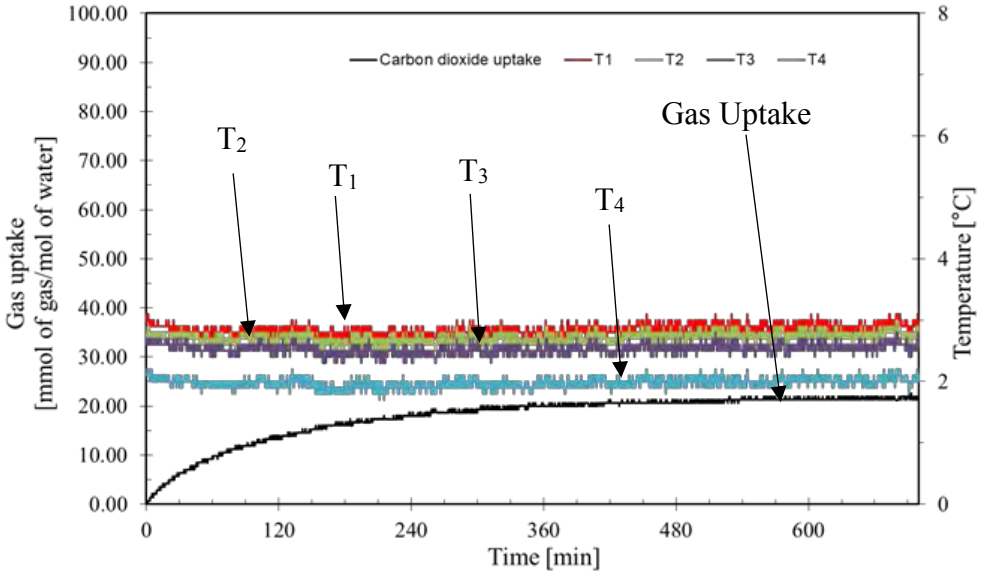

Figure 4.7 CO_2 hydrate formation experiment at 3 °C and 3 MPa in the presence of 2.28 mM of SDS (Experiment No.13).

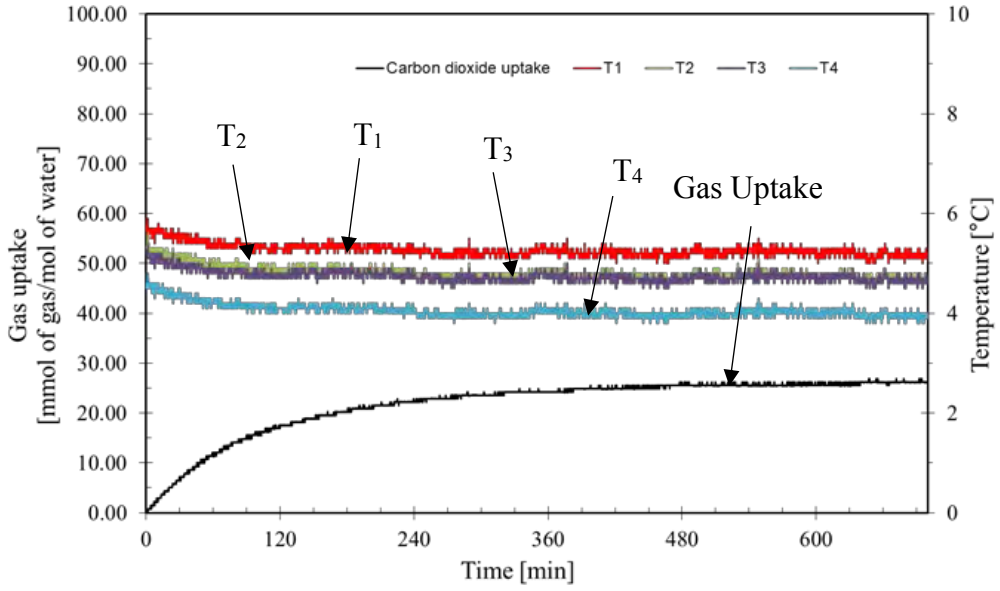

Figure 4.8 CO_2 hydrate formation experiment at 3 °C and 3 MPa in the presence of 4 mM of SDS (Experiment No.14).

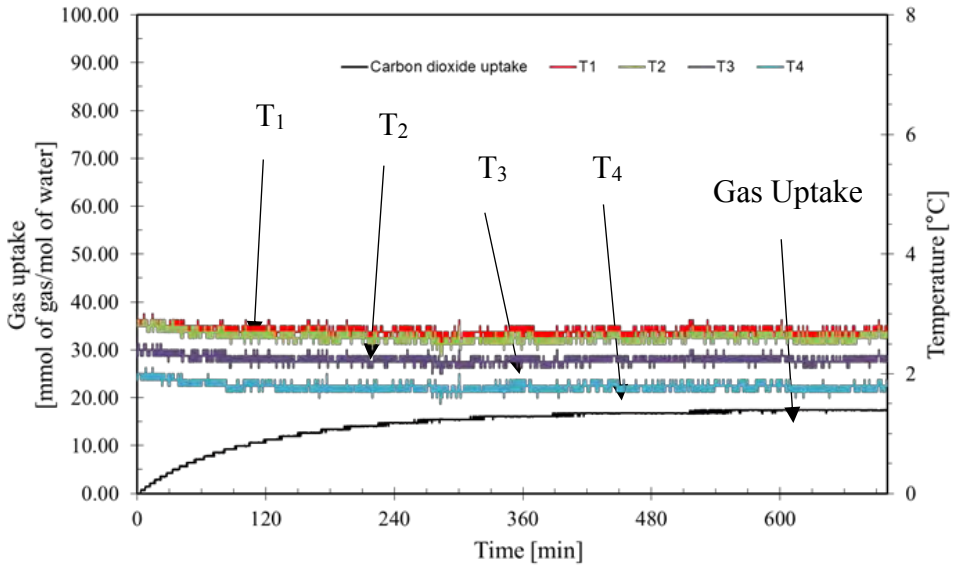

Figure 4.9 CO_2 hydrate formation experiment at 3 °C and 3 MPa in the presence of 8.2 mM of SDS (Experiment No.17).

4.2 Effects of Mixed Promoters

4.2.1 Effects of Methyl Ester Sulfonate (MES) and of Tetrahydrofuran (THF)

4.2.1.1 With 5.56 mol% THF

- CO_2 Hydrate Formation

Figure 4.10 shows the formation of CO_2 hydrates in the presence of 2 mM MES and 5.56 mol% THF. CO_2 hydrates form as seen from the temperature spikes that dramatically increase almost the same time. The temperature changes at the interphase, T_1 and T_2, take place before the changes at the other two locations, T_3 and T_4. This indicates that the hydrates formed at the interphase first. The results are also consistent with the report by Kumar *et al*., (2015). Figure 4.11 shows the CO_2 hydrate formation in the presence of 3 mM MES and 5.56 mol% THF. The temperature profile are relatively different from 2 mM MES and 5.56 mol% THF. The temperature dramatically increases only T_1 and T_2, which are the interphase temperature between gas phase and liquid phase. This again confirms the formation at the interphase first, and the interphase hydrates block further gas consumed. Thereby, CO_2 consumed in the presence of 3 mM MES and 5.56 mol% THF is less than 2 mM MES and 5.56 mol% THF. As the concentration of surfactant increases to 4 mM MES

with 5.56 mol% THF, the results show that gas uptake decreases with no hydrate formation, Figure 4.12. Although the presence of surfactant decreases the surface tension and increase the solubility of gas, increasing the amount of MES in the 5.56 mol% THF solution decreases the gas uptake and could somehow inhibit the formation (Chaturvedi *et al.*, 2018). Nevertheless, the amount of CO_2 consumed and the induction time of hydrate formation in the presence of 2, 3, and 4 mM MES with 5.56 mol% THF are shown in Table 4.5.

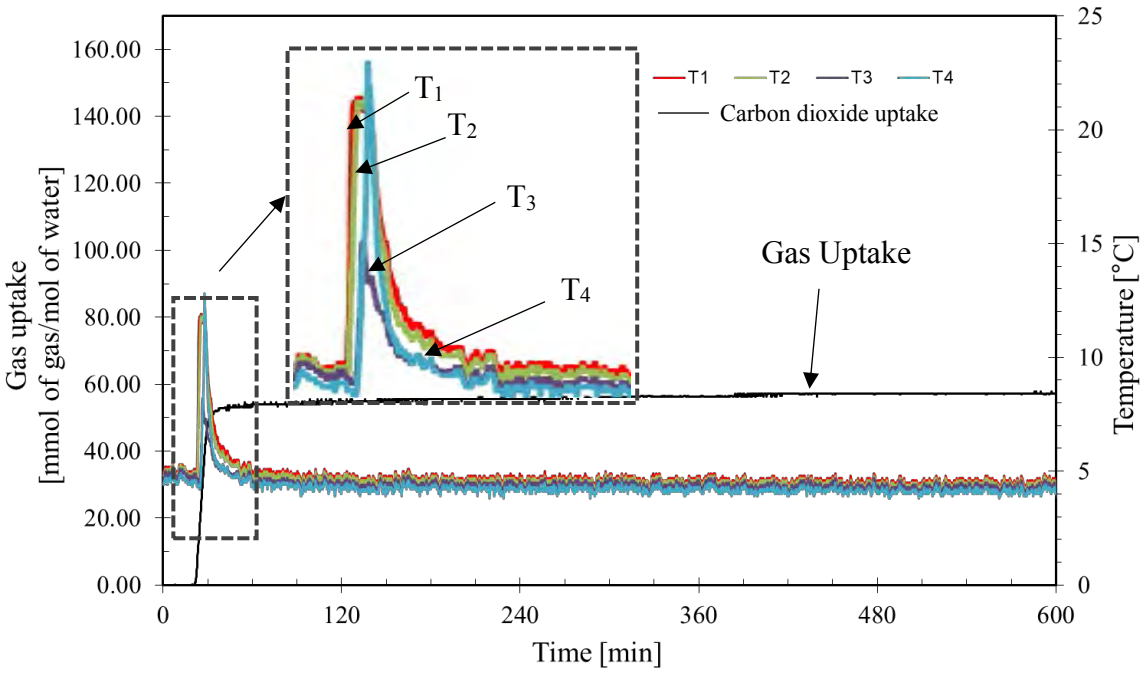

Figure 4.10 CO_2 hydrate formation experiment at 3 °C and 3 MPa in the presence of 2 mM of MES and 5.56 mol% THF (Experiment No.19).

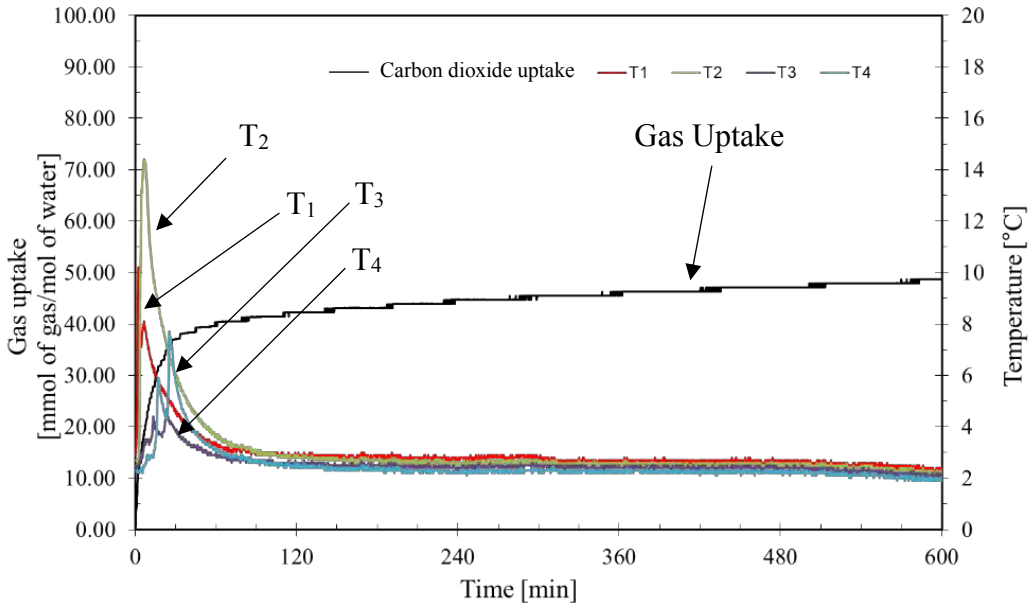

Figure 4.11 CO_2 hydrate formation experiment at 3 °C and 3 MPa in the presence of 3 mM of MES and 5.56 mol% THF (Experiment No.21).

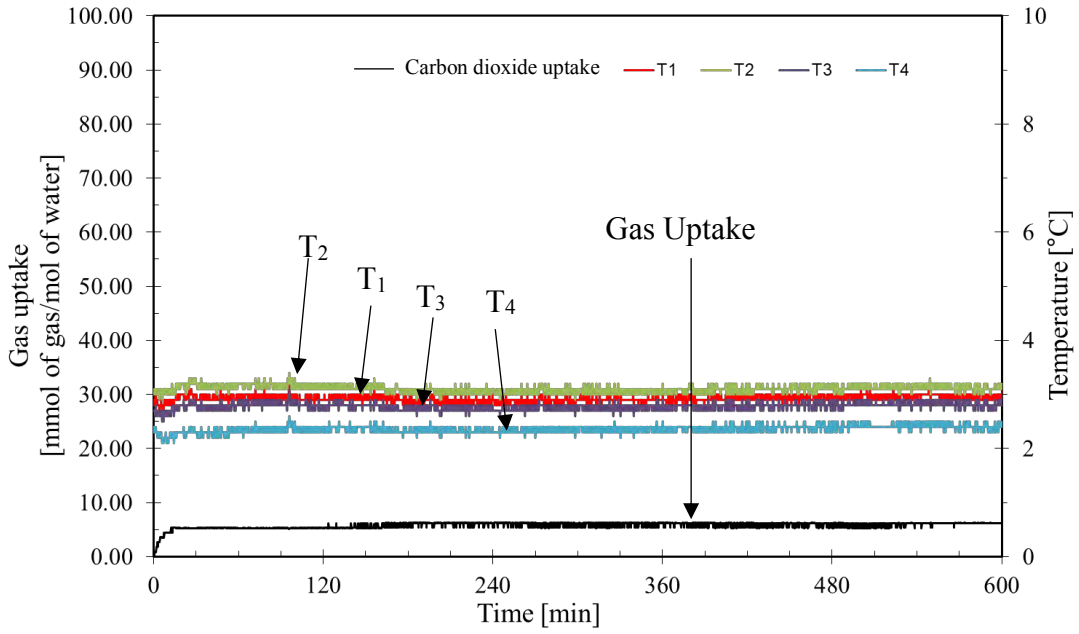

Figure 4.12 CO_2 hydrate formation experiment at 3 °C and 3 MPa in the presence of 4 mM of MES and 5.56 mol% THF (Experiment No.24).

Table 4.5 CO_2 hydrate formation experiments with the presence of 2, 3, and 4 mM MES and 5.56 mol% THF

Exp.	Promoter compositions	[a]Induction time (min)	CO_2 consumed (mmol/mol of water)
	Water	[b]	-
18	2 mM MES + 5.56 mol% THF	10.50	51.82
19	2 mM MES + 5.56 mol% THF	23.33	58.71
20	2 mM MES + 5.56 mol% THF	48.83	52.23
		Average	54.25 ± 3.86
21	3 mM MES + 5.56 mol% THF	0.83	50.24
22	3 mM MES + 5.56 mol% THF	533	42.99
		Average	46.62 ± 5.13
23	4 mM MES + 5.56 mol% THF	[b]	6.21
24	4 mM MES + 5.56 mol% THF	[b]	0.83
		Average	3.52 ± 3.80

[a]Induction Time = time at the first hydrate formation

[b]No CO_2 hydrates formed during 13 hours of the experiment

- CO_2 Hydrate Dissociation

The CO_2 released and recovery from the hydrates are shown in Table 4.6. CO_2 released from the hydrates formed with 2 mM MES and 5.56 mol% THF is higher than that with 3 mM MES and 5.56 mol% THF. That may be associated with the higher gas uptake of the system with 2 mM MES and 5.56 mol% THF than 3 mM MES and 5.56 mol% THF. In addition, the CO_2 recovery also depends on the promoter added during the formation.

Figures 4.13 - 4.14 present the gas released and temperature profiles from the hydrates formed in the presence of 2 mM MES and 5.56 mol% THF at 3 mM and 5.56 mol% THF. The gas released in the presence of 2 mM MES and 5.56 mol % THF start around 10 °C. On the contrary, with 3 mM MES and 5.56 mol% THF, the gas releases slowly for the first 50 min before reaching a plateau. The hydrate dissociation depends on the heat transfer and mass transfer. The ability to reduce the surface tension and increase mass transfer between gas and liquid of MES affect the amount of CO_2 released and the final recovery.

Table 4.6 CO_2 Hydrate dissociation experiments for the hydrates formed with 2 and 3 mM MES with 5.56 mol% THF at 35 °C

Exp.	Promoter compositions	CO_2 released (mmol/mol of water)	CO_2 recovery (mol%)
18	2 mM MES + 5.56 mol% THF	44.5	65.16
19	2 mM MES + 5.56 mol% THF	44.46	57.52
20	2 mM MES + 5.56 mol% THF	16.33	23.60
	Average	35.10 ± 16.25	48.76 ± 22.12
21	3 mM MES + 5.56 mol% THF	22.25	34.08
22	3 mM MES + 5.56 mol% THF	22.21	39.23
	Average	22.23 ± 0.03	36.66 ± 3.64

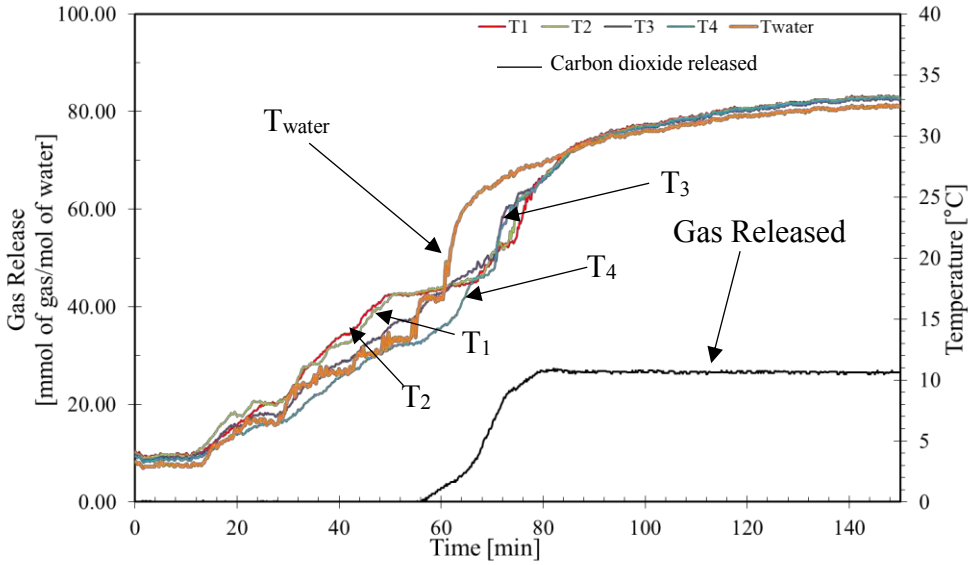

Figure 4.13 Dissociation of CO_2 hydrates formed in the presence of 2 mM MES and 5.56 mol% THF (Experiment No.19).

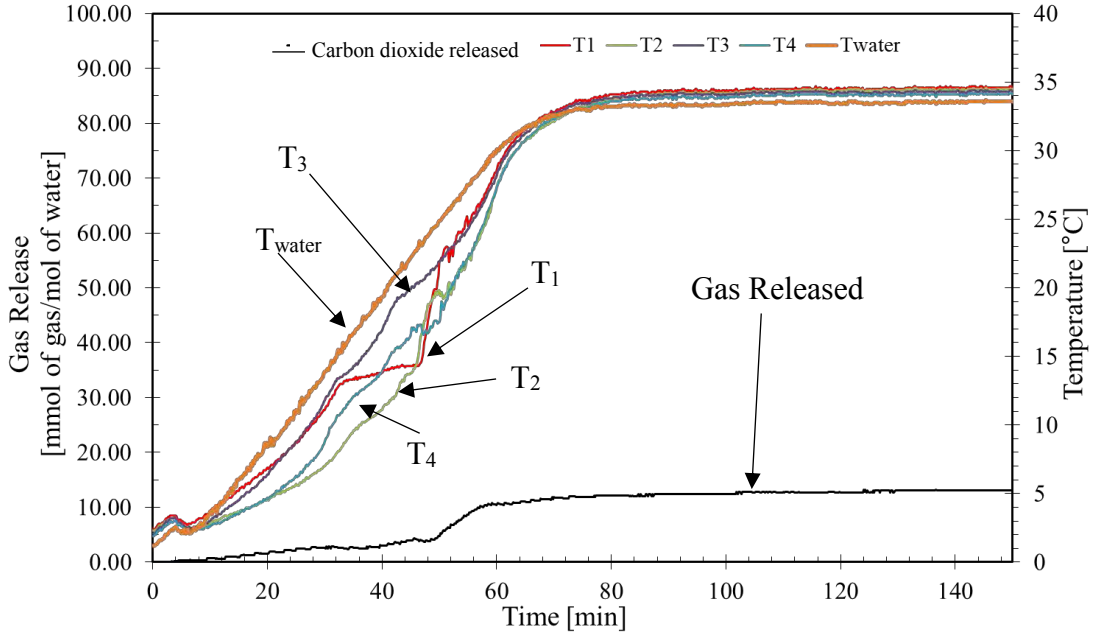

Figure 4.14 Dissociation of CO_2 hydrates formed in the presence of 3 mM MES and 5.56 mol% THF (Experiment No.21).

4.2.1.2 With 4.50 mol% THF

- CO_2 Hydrate Formation

The gas uptakes in the presence of 2 and 4 mM MES with 4.50 mol% THF are shown in Table 4.7. The hydrates form in the presence of 4 mM MES and 4.50 mol% THF, while no hydrates form in the presence of 4 mM MES and 5.56 mol% THF. That is because MES micelles obstructed the hydrate formation in the presence of 5.56 mol% THF, which is the stoichiometric ratio to form structure II hydrates. Moreover, the structure I hydrates could form easier than structure II as seen in Figure 2.8. Therefore, the results imply that the hydrates could form in the presence of 4.5 mol% THF by occupying the structure I.

The temperature profiles and gas uptakes during the CO_2 hydrate formation in the presence of 2 mM MES and 4.50 mol% THF are in Figure 4.15. The results indicate that the hydrates form in every location at the same time. However, the temperature profiles of CO_2 hydrate formation in the presence of 4 mM MES and 4.50 mol% THF show that the temperature at the interphase (T_1) dramatically increases first, followed by T_2, T_3, and T_4, respectively, as shown in Figure 4.16. This indicates that the hydrates form from the interphase first.

- CO_2 Hydrate Dissociation

Table 4.8 shows the CO_2 released and recovery in the presence of 2 and 4 mM MES with 4.50 mol% THF. The CO_2 released in the presence of 4 mM MES and 4.50 mol% THF is about the same as that with 2 mM MES and 4.50 mol% THF because the synergistic effect of MES and 4.50 mol% THF.

The temperature profiles and the CO_2 released in the presence of 2 and 4 mM MES with 4.5 mol% THF are shown in Figures 4.17 and 4.18, respectively. Both figures show the gas first releases around 5 °C and again at 15 °C.

Table 4.7 CO_2 hydrate formation experiments with the presence of 2 and 4 mM MES and 4.50 mol% THF

Exp.	Promoter compositions	[a]Induction time (min)	CO_2 consumed (mmol/mol of water)
	Water	[b]	-
25	2 mM MES + 4.50 mol% THF	199	56.75
26	2 mM MES + 4.50 mol% THF	168.67	39.7
		Average	48.23 ± 12.06
27	4 mM MES + 4.50 mol% THF	11.17	52.40
28	4 mM MES + 4.50 mol% THF	31.17	34.80
29	4 mM MES + 4.50 mol% THF	7.5	47.20
		Average	44.80 ± 9.04

[a]Induction Time = time at the first hydrate formation

[b]No CO_2 hydrates formed during 13 hours of the experiment

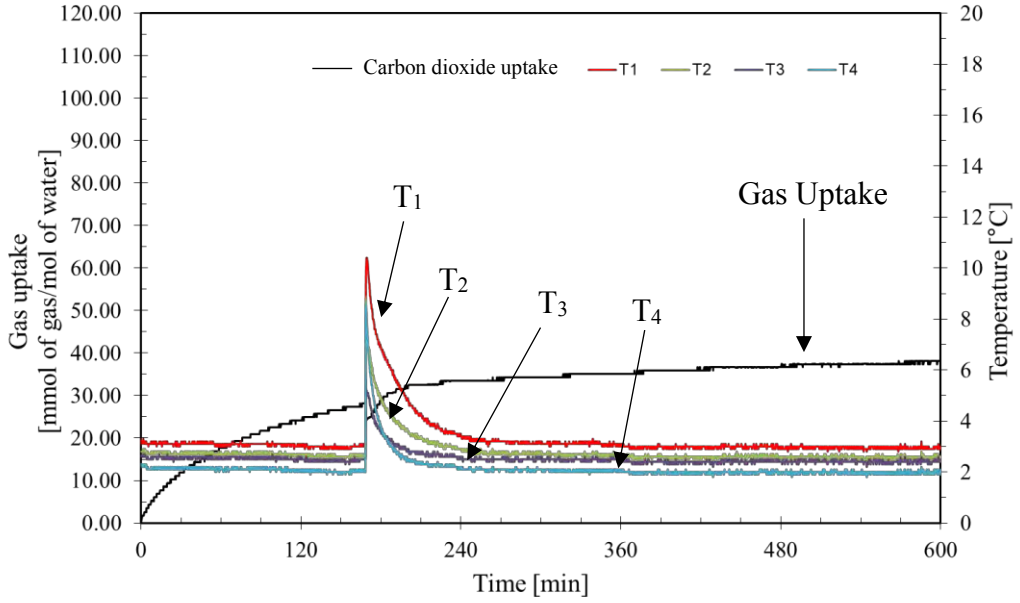

Figure 4.15 CO_2 hydrate formation experiment at 3 °C and 3 MPa in the presence of 2 mM of MES and 4.50 mol% THF (Experiment No.26).

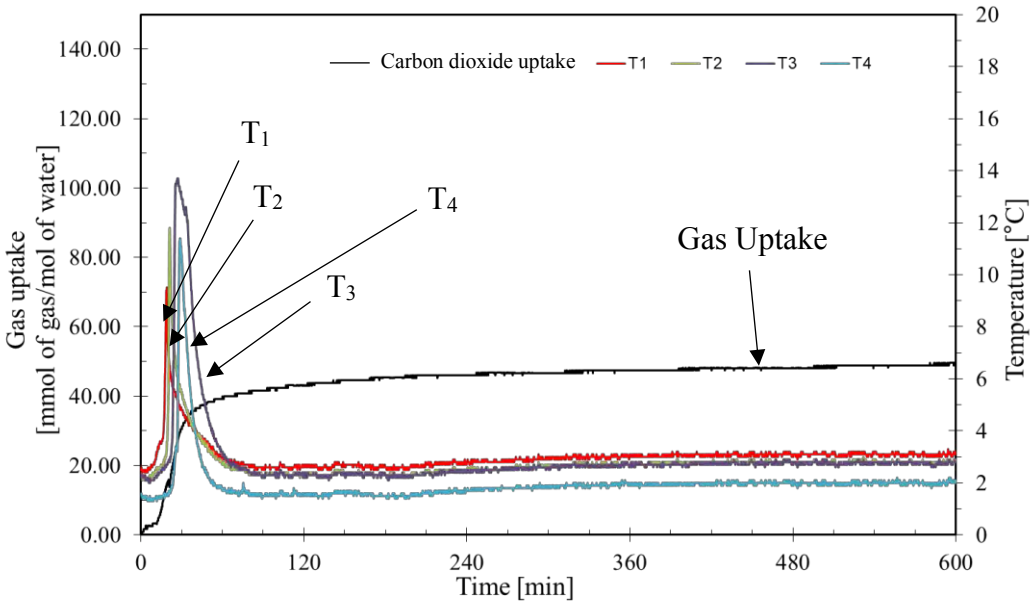

Figure 4.16 CO_2 hydrate formation experiment at 3 °C and 3 MPa in the presence of 4 mM of MES and 4.50 mol% THF (Experiment No.29).

Table 4.8 CO_2 Hydrate dissociation experiments for hydrates formed with 2 mM MES and 4.50 mol% THF at 35 °C

Exp.	Promoter compositions	CO_2 released (mmol/mol of water)	CO_2 recovery (mol%)
25	2 mM MES + 4.50 mol% THF	39	49.87
26	2 mM MES + 4.50 mol% THF	25.98	47.5
	Average	32.49 ± 9.21	48.69 ± 1.68
27	4 mM MES + 4.50 mol% THF	37.52	51.97
28	4 mM MES + 4.50 mol% THF	32.79	68.39
29	4 mM MES + 4.50 mol% THF	34.37	50.45
	Average	34.37 ± 2.73	56.94 ± 9.94

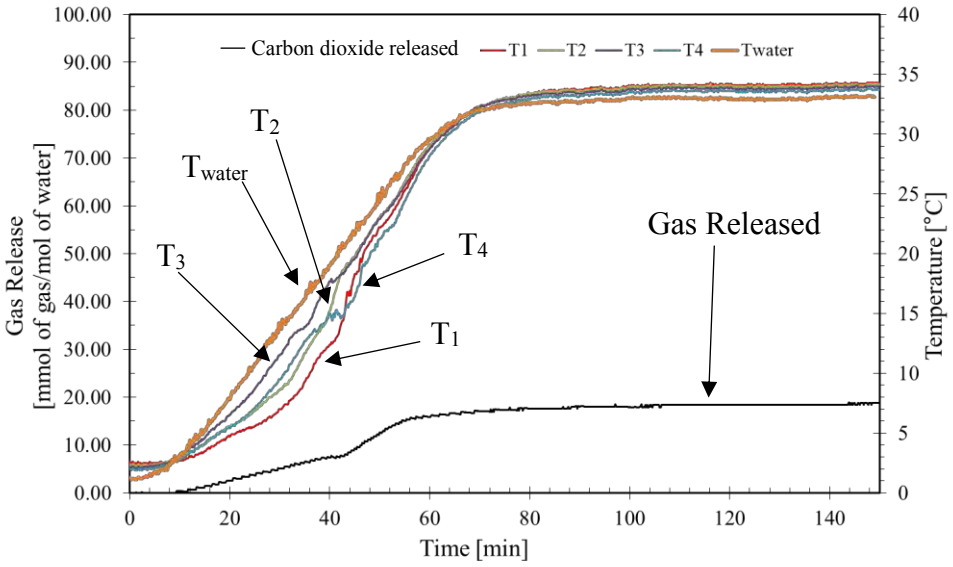

Figure 4.17 Dissociation of CO_2 hydrates formed in the presence of 2 mM MES and 4.50 mol% THF (Experiment No.26).

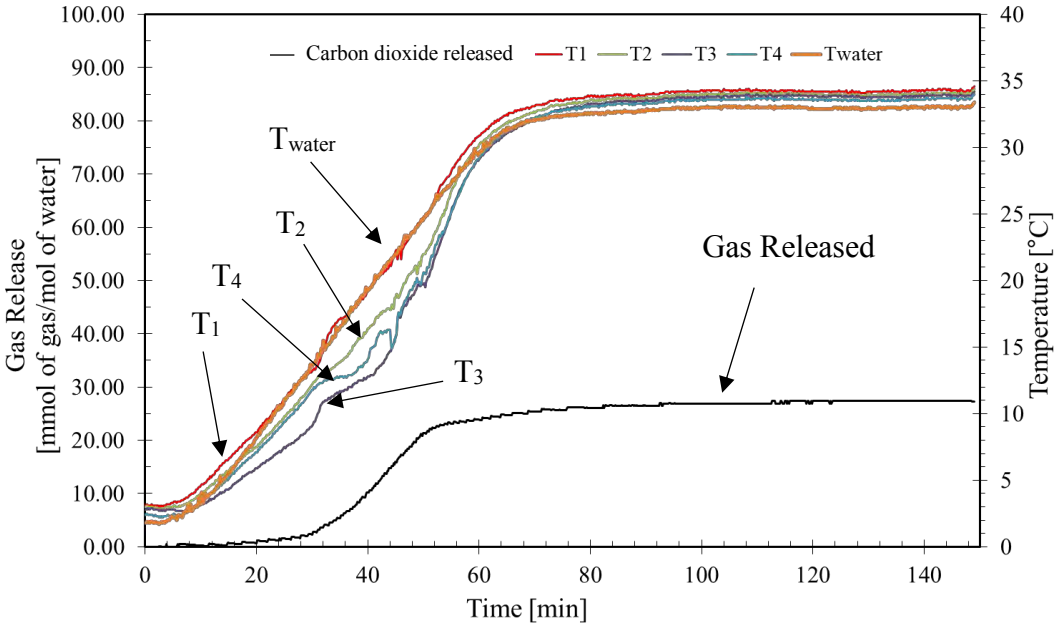

Figure 4.18 Dissociation of CO_2 hydrates formed in the presence of 4 mM MES and 4.50 mol% THF (Experiment No.27).

Figure 4.19 shows the CO_2 consumed during the hydrate formation in the presence of mixed promoters with different concentrations. It is clear that 2 mM MES is very efficient with both 4.50 and 5.56 mol% THF, and especially for 2 mM MES and 5.56 mol% THF. The comparison of gas consumed between the same amount of MES, 2 mM, and different concentrations of THF are about the same. Therefore, it is the synergistic effect between MES and THF by reducing the surface tension with MES and enhancing the hydrate formation condition with THF.

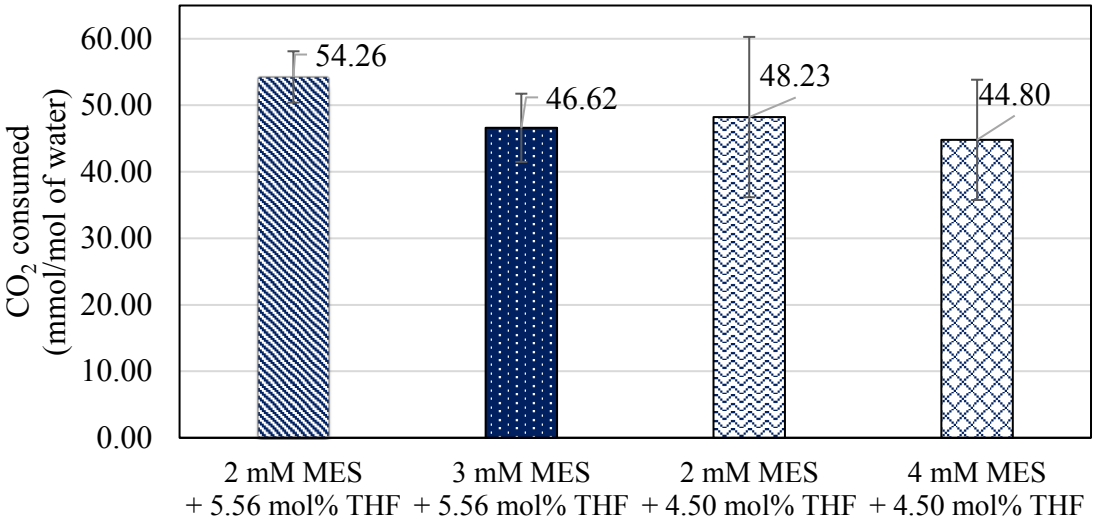

Figure 4.19 The CO_2 consumed in presence of mixed promoters between methyl ester sulfonate (MES) and tetrahydrofuran (THF) with different concentration.

4.2.2 Effect of Sodium Dodecyl Sulfate (SDS) and Tetrahydrofuran (THF)

4.2.2.1 With 5.56 mol% THF

- CO_2 Hydrate Formation

Table 4.9 shows the results from CO_2 hydrate formation experiments in the presence of 2.28, 4, and 8.2 mM MES with 5.56 mol% THF. The hydrates could from in the presence of 2.28 and 4 mM SDS with 5.56 mol% THF but could not form in the presence of 8.2 mM MES and 5.56 mol% THF. Kumar *et al.* (2015) purposed the possible explanations that THF and SDS are jointly very efficient in quiescent conditions. It may be that the actions of two promoters provide a porous texture to the hydrates formed in bulk, which can permeate CO_2. They also explained two possible mechanisms that SDS can reduce the induction and enhance the gas uptake. The interfacial tension of gas-liquid decreases after dodecyl sulfate anions (DS^-) are adsorbed. Another reason is hydrate formers such as methane or THF are solubilized in the hydrophobic domains formed by adsorbed DS^-, which increase the concentration of hydrate formers at the solution interface. Therefore, the synergistic effect of THF and SDS can be observed in the experiment.

Figures 4.20 – 4.21 show the temperature all of thermocouples dramatically increase due to the hydrates form at the same time at all

locations. In addition, Figure 4.22 shows the constant temperature as there is no hydrate formation.

Table 4.9 CO_2 hydrate formation experiments with the presence of 2.28, 4, and 8.2 mM SDS and 5.56 mol% THF

Exp.	**Promoter compositions**	**[a]Induction time (min)**	**CO_2 consumed (mmol/mol of water)**
	Water	[b]	-
30	2.28 mM SDS + 5.56 mol% THF	0.17	48.27
31	2.28 mM SDS + 5.56 mol% THF	24.17	20.54
		Average	34.41 ± 19.61
32	4 mM SDS + 5.56 mol% THF	0.17	43.27
33	4 mM SDS + 5.56 mol% THF	325	57.21
34	4 mM SDS + 5.56 mol% THF	347	58.81
		Average	53.10 ± 8.57
35	8.2 mM SDS + 5.56 mol% THF	[b]	2.60
36	8.2 mM SDS + 5.56 mol% THF	[b]	6.17
		Average	4.39 ± 2.52

[a]Induction Time = time at the first hydrate formation

[b]No CO_2 hydrates formed during 13 hours of the experiment

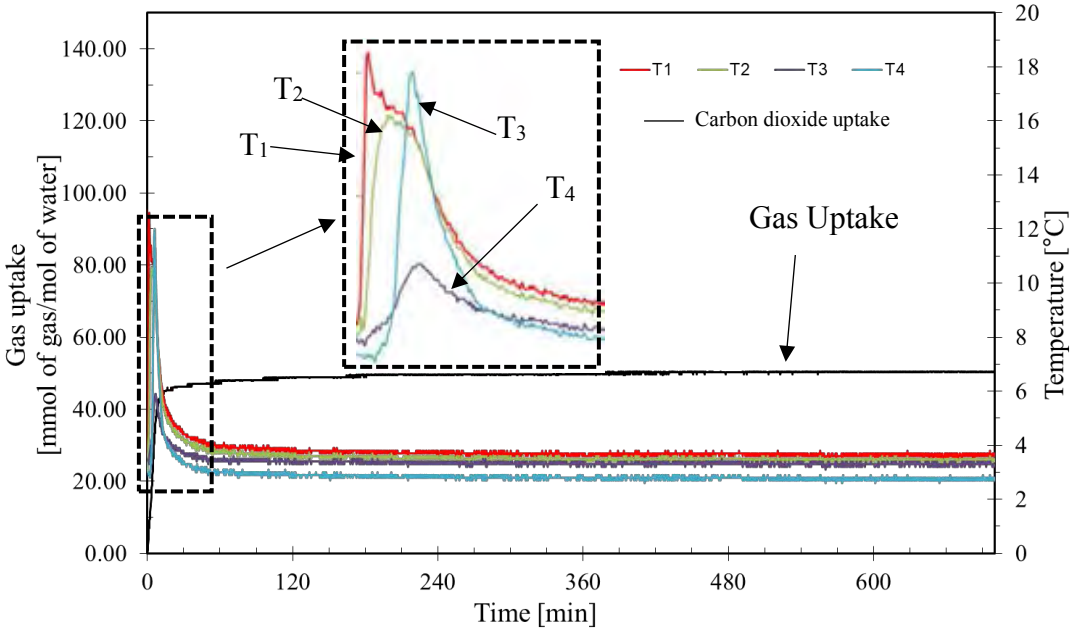

Figure 4.20 CO_2 hydrate formation experiment at 3 °C and 3 MPa in the presence of 2.28 mM of SDS and 5.56 mol% THF (Experiment No.30).

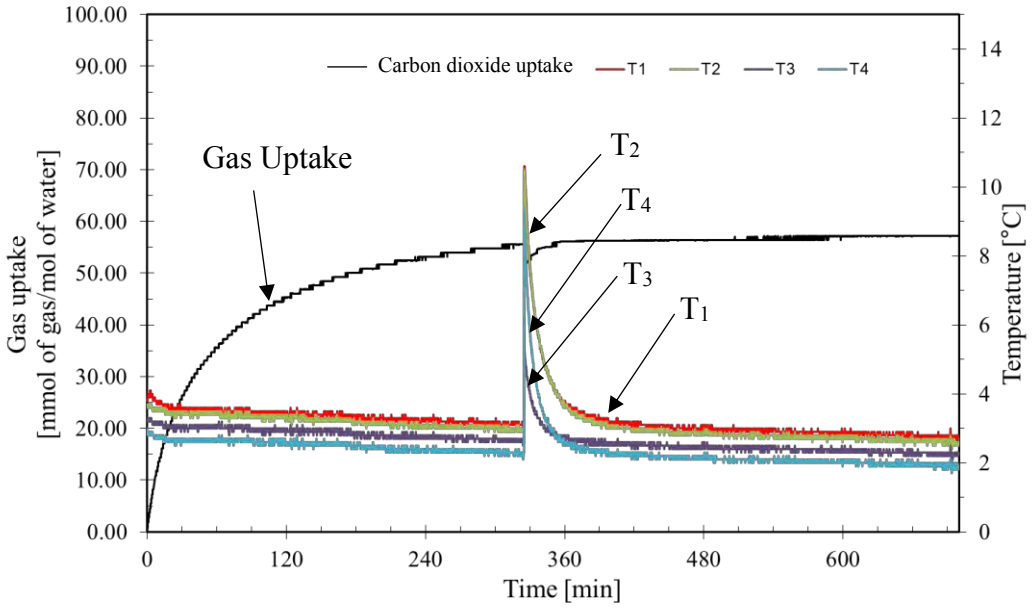

Figure 4.21 CO_2 hydrate formation experiment at 3 °C and 3 MPa in the presence of 4 mM of SDS and 5.56 mol% THF (Experiment No.33).

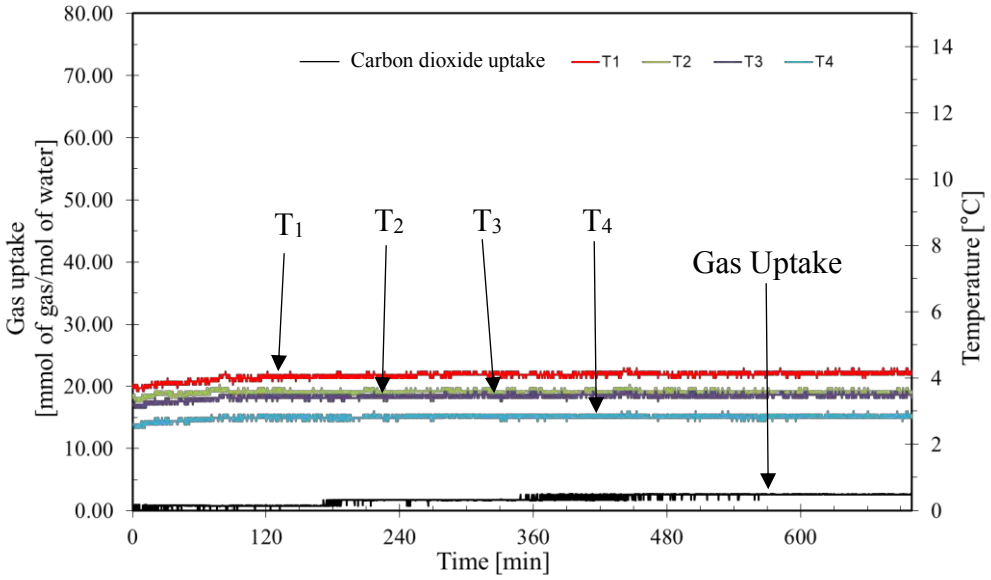

Figure 4.22 CO_2 hydrate formation experiment at 3 °C and 3 MPa in the presence of 8.2 mM of SDS and 5.56 mol% THF (Experiment No.35).

- CO_2 Dissociation

Table 4.10 shows that CO_2 released form the hydrates formed in the presence of 4 mM SDS and 5.56 mol% THF is higher than in the presence of 2.28 mM SDS and 5.56 mol% THF. For CO_2 recovery, the hydrates formed with low SDS concentration is higher than the other because there is more foam with higher SDS concentration. The gas released in the presence of 2.28 mM SDS and 5.56 mol% THF increases slowly, as shown in Figure 4.23. Figure 4.24 shows gas released around 15 °C in the presence of 4 mM SDS and 5.56 mol% THF.

Table 4.10 CO_2 Hydrate dissociation experiment for hydrates formed with 2.28 and 4 mM SDS and 5.56 mol% THF at 35 °C

Exp.	Promoter compositions	CO_2 released (mmol/mol of water)	CO_2 recovery (mol%)
30	2.28 mM SDS + 5.56 mol% THF	26.57	40.08
31	2.28 mM SDS + 5.56 mol% THF	15.96	59.02
	Average	21.27 ± 7.5	49.55 ± 13.39
32	4 mM SDS + 5.56 mol% THF	35.78	56.31
33	4 mM SDS + 5.56 mol% THF	22.97	30.49
34	4 mM SDS + 5.56 mol% THF	26.18	33.81
	Average	28.31 ± 6.67	40.20 ± 14.05

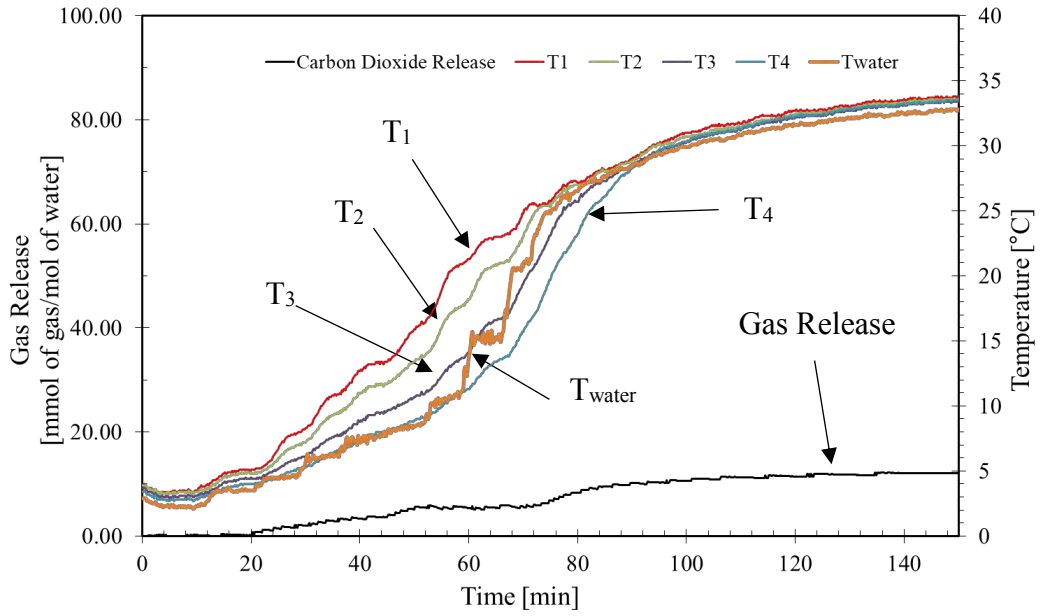

Figure 4.23 Dissociation of CO_2 hydrates formed in the presence of 2.28 mM SDS and 5.56 mol% THF (Experiment No.31).

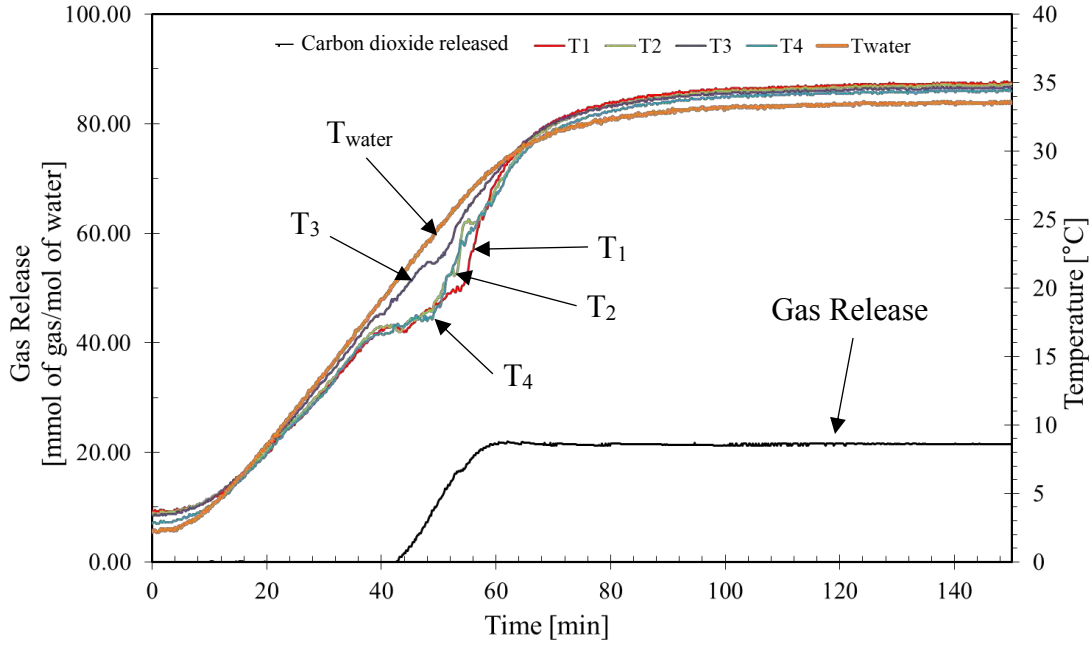

Figure 4.24 Dissociation of CO_2 hydrates formed in the presence of 4 mM SDS and 5.56 mol% THF (Experiment No.32).

4.2.2.2 With 4.50 mol% THF

- CO_2 Hydrate Formation

The CO_2 hydrate formation experiments in the presence of 2.28, 4, and 8 mM with 4.50 mol% THF are shown in Table 4.11. The CO_2 hydrates form in the presence of 8.2 mM with 4.50 mol% THF. Conversely, the hydrates do not form in the presence of 8.2 mM MES with 5.56 mol% THF. For 5.56 mol% THF, the hydrates could form only structure II, and the SDS micelles would obstruct the hydrate formation. The results show that, in the presence of 4.50 mol% THF, the hydrates form with structure I because the structure I is easier to form than the structure II. Nevertheless, CO_2 hydrates could not form in the presence of 2.28 mM SDS and 4.50 mol% THF.

Figure 4.25 shows no temperature spike and also small amount of gas uptake due to no hydrate formation in the presence of 2.28 mM SDS and 4.5 mol% THF. Figures 2.26 – 2.27 show the temperature profiles and gas uptake in the presence of 4 and 8.2 mM SDS with 4.50 mol% THF. The temperature profiles show that the temperatures rapidly increase at the same time then decrease to the water temperature.

- CO_2 Hydrate Dissociation

CO_2 released and recovery of CO_2 hydrate dissociation in the presence of 4 and 8.2 mM SDS with 4.5 mol% THF are shown in Table 4.12. CO_2 released from the hydrates formed in the presence of 4 and 8.2 mM SDS with 4.5 mol% are almost the same. Therefore, in the presence of 4.50 mol% THF does not affect on the CO_2 released.

Temperature profiles and the gas released in the presence of 4 and 8.2 mM SDS with 4.50 mol% THF are shown in Figures 4.28 – 4.29. Both figures show the same behavior of the temperature profile and gas released, which is around 5 °C and 12 °C.

Table 4.11 CO_2 hydrate formation experiments with the presence of 2.28, 4, and 8.2 mM SDS and 4.50 mol% THF

Exp.	Promoter compositions	[a]Induction time (min)	CO_2 consumed (mmol/mol of water)
	Water	[b]	-
37	2.28 mM SDS + 4.50 mol% THF	[b]	5.5
38	2.28 mM SDS + 4.50 mol% THF	[b]	11.8
		Average	8.65 ± 4.46
39	4 mM SDS + 4.50 mol% THF	134	26.12
40	4 mM SDS + 4.50 mol% THF	37.17	41.66
		Average	33.89 ± 10.99
41	8.2 mM SDS + 4.50 mol% THF	92.83	34.69
42	8.2 mM SDS + 4.50 mol% THF	0.17	37.94
		Average	36.32 ± 2.30

[a]Induction Time = time at the first hydrate formation

[b]No CO_2 hydrates formed during 13 hours of the experiment

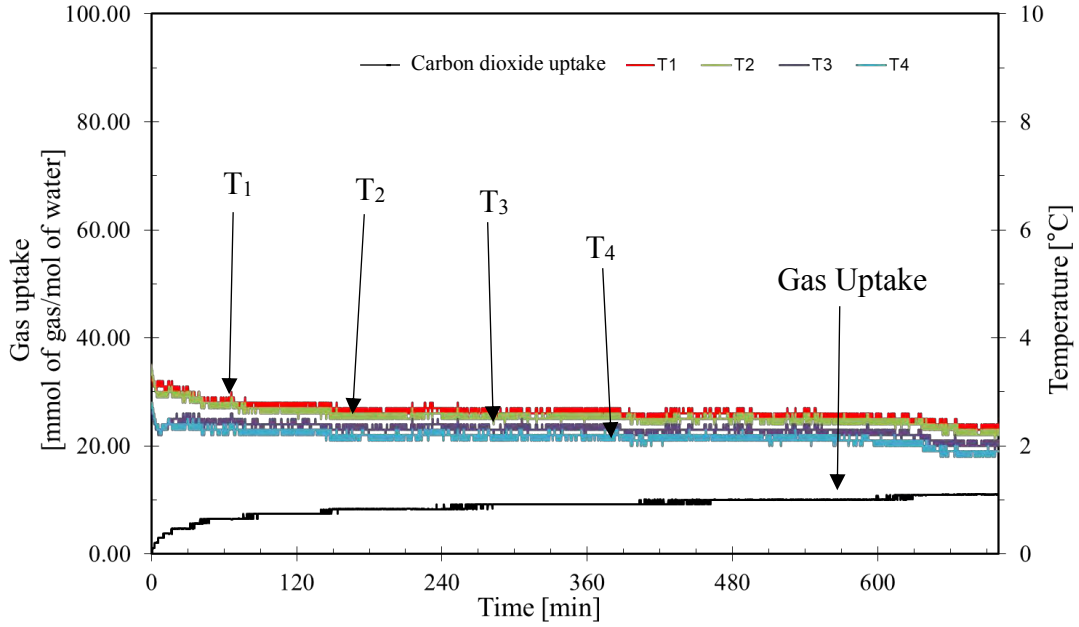

Figure 4.25 CO_2 hydrate formation experiment at 3 °C and 3 MPa in the presence of 2.28 mM of SDS and 4.50 mol% THF (Experiment No.38).

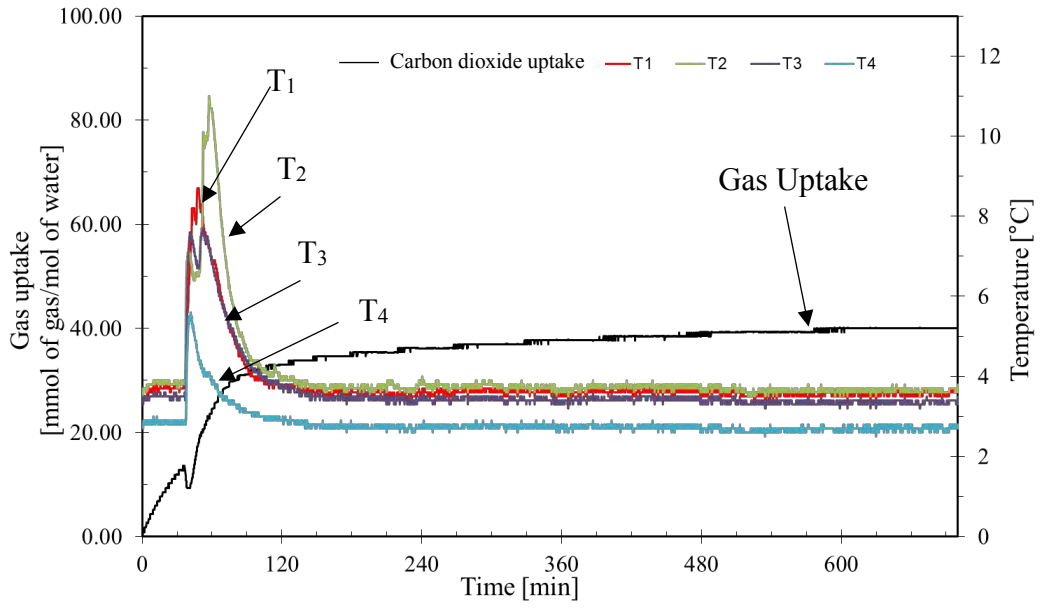

Figure 4.26 CO_2 hydrate formation experiment at 3 °C and 3 MPa in the presence of 4 mM of SDS and 4.50 mol% THF (Experiment No.40).

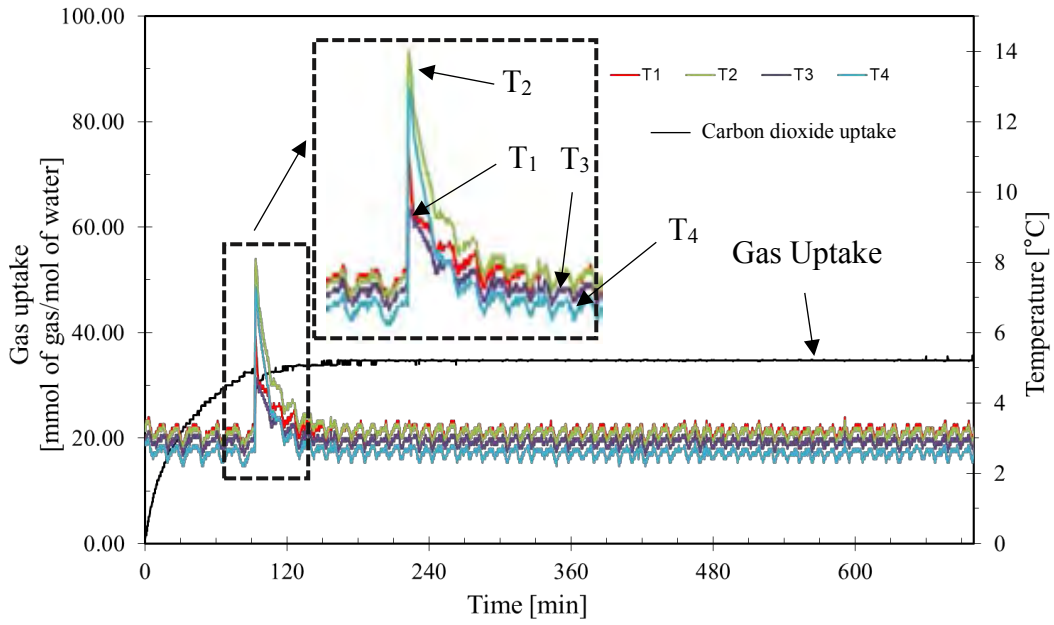

Figure 4.27 CO_2 hydrate formation experiment at 3 °C and 3 MPa in the presence of 8.2 mM of SDS and 4.50 mol% THF (Experiment No.41).

Table 4.12 CO_2 Hydrate dissociation experiments for hydrates formed with 4 and 8.2 mM SDS and 4.50 mol% THF at 35 °C

Exp.	Promoter compositions	CO_2 released (mmol/mol of water)	CO_2 recovery (mol%)
39	4 mM SDS + 4.50 mol% THF	16.76	35.98
40	4 mM SDS + 4.50 mol% THF	28.39	49.47
	Average	22.58 ± 8.22	42.725 ± 9.54
41	8.2 mM SDS + 4.50 mol% THF	19.92	41.69
42	8.2 mM SDS + 4.50 mol% THF	21.46	41.05
	Average	20.69 ± 1.09	41.37 ± 0.45

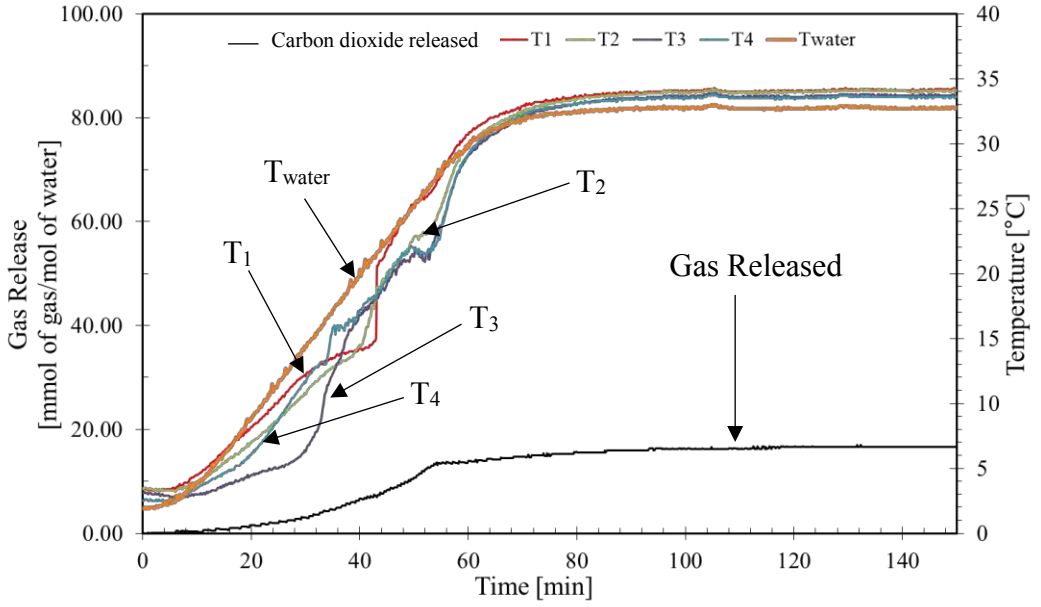

Figure 4.28 Dissociation of CO_2 hydrates formed in the presence of 4 mM SDS and 4.50 mol% THF (Experiment No.40).

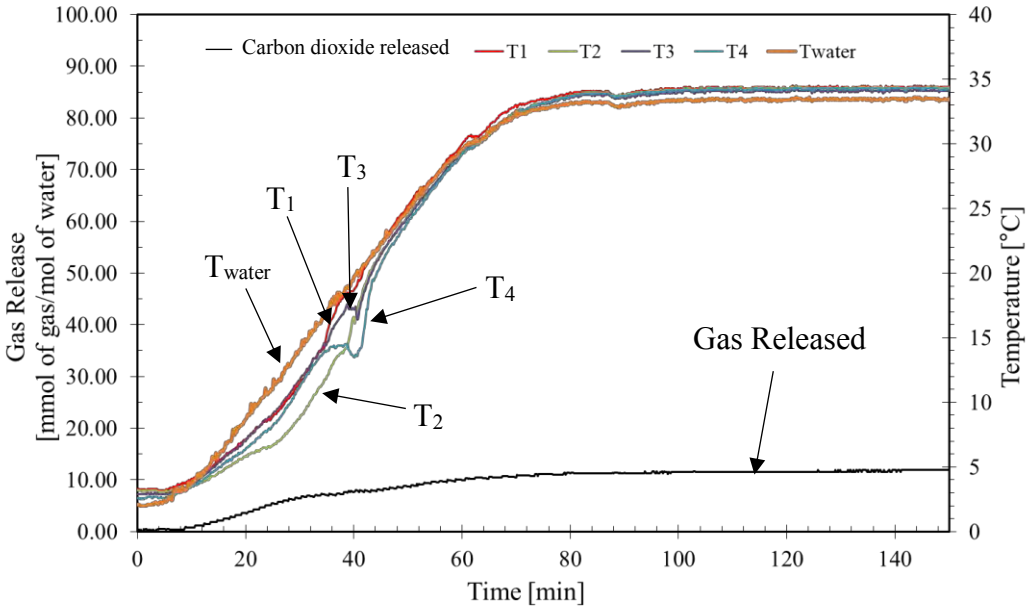

Figure 4.29 Dissociation of CO_2 hydrates formed in the presence of 8.2 mM SDS and 4.50 mol% THF (Experiment No.41).

Figure 4.30 shows the CO_2 consumed with different concentrations of SDS mixed with THF. The figure shows that using the mixture of 4 mM SDS and 5.56 mol% THF result in the highest gas uptake.

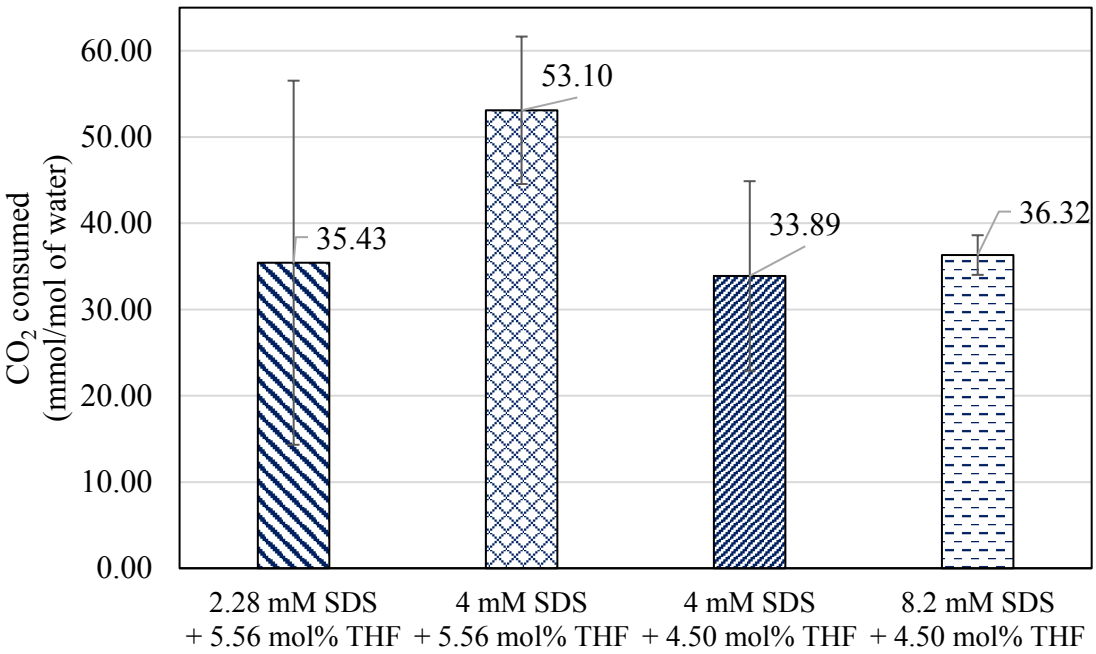

Figure 4.30 The CO_2 consumed in presence of mixed promoters between sodium dodecyl sulfate (SDS) and tetrahydrofuran (THF) with different concentration.

CHAPTER V
CONCLUSIONS AND RECOMMENDATIONS

5.1 Conclusions

In this work, the CO_2 hydrate formation was studied with tetrahydrofuran (THF), sodium dodecyl sulfate (SDS), and methyl ester sulfonate (MES). The hydrate formation was carried out in the quiescent close system at 3°C and 3 MPa. The CO_2 hydrates formed in the presence of 10 mol% THF, while it did not form in the presence of 4.50 and 5.56 mol% THF. It may be concluded that the concentration lower than 10 mol% THF hardly promoted the hydrate formation during 13 hours. Even though SDS or MES decreased the surface tension between the gas-liquid phase, the CO_2 hydrates did not form. In the quiescent close system at 3°C and 3 MPa, the presence of surfactants was not sufficient to promote CO_2 hydrate formation. The synergistic effects of THF and both surfactants were investigated at their CMCs. This study found that the CO_2 hydrates could form in the presence of 4.50 mol% THF with CMCs, while it could not form in the presence of 5.56 mol% THF with CMC point. The mixtures of 4.50 or 5.56 mol% THF and either surfactant promoted CO_2 hydrate formation and resulted in higher CO_2 consumed than in the presence of 10 mol% THF and the surfactants.

5.2 Recommendation

Based on the experiment that has been discovered in this study, the recommendation is to study the CO_2 hydrate formation and dissociation at other conditions.

REFFERENCES

Aman, Z.M. and Koh, C.A. (2016). Interfacial Phenomena in Gas Hydrate Systems. The Royal Society of Chemistry 45(6), 1678-1690.

Anthony, D.,Fournaison, L.,Marinhas, S.,Chatti, I.,Petitet, J.-P.,Dalmazzone, D., and Furst, W. (2006). Effect of THF on Equilibrium Pressure and Dissociation Enthalpy of CO_2 Hydrates Applied to Secondary Refrigeration. Industrial and Engineering Chemistry Research 45, 391-397.

Chaturvedi, E.,Prasad, N., and Mandal, A. (2018). Enhanced Formation of Methane Hydrate Using a Novel Synthesized Anionic Surfactant for Application in Storage and Transportation of Natural Gas. Journal of Natural Gas Science and Engineering 56, 246-257.

Davis, W. (2017). The Relationship between Atmospheric Carbon Dioxide Concentration and Global Temperature for the Last 425 Million Years. Climate 5(4), 76-111.

Getachew, M.A. and Gizaw, M.T. (2018). Comparison of CO_2 from NOAA Carbon Tracker Reanalysis Model and Satellites Over Africa. Atmospheric Measurement Techniques Discussions 84, 1-31.

Johnny, D. and Didier, D. (2009). Dissociation Enthalpies and Phase Equilibrium for TBAB Semi-clathrate Hydrates of N_2, CO_2, $N_2 + CO_2$ and $CH_4 + CO_2$. Journal of Thermal Analysis and Calorimetry 98(1), 113-118.

Kazunori, O.,Yui, K., and H., M.Y. (2008). Surfactant Effects on Hydrate Formation in an Unstirred Gas/Liquid System: An Experimental Study Using Methane and Sodium Alkyl Sulfates. Chemical Engineering Science 63(1), 183-194.

Kumar, A.,Bhattacharjee, G.,Kulkarni, B.D., and Kumar, R. (2015). Role of Surfactants in Promoting Gas Hydrate Formation. Industrial & Engineering Chemistry Research 54(49), 12217-12232.

Kumar, M.M.,Kumar, B.H., and Prachi, V. (2012). Progress and Trends in CO_2 Capture/Separation Technologies: A review. Energy 46(1), 431-441.

Kvamme, B. (2002). Kinetics of Hydrate Formation From Nucleation Theory. International Journal of Offshore and Polar Engineering 12(4), 256-263.

Lele, J.,Airong, L.,Jingfan, X., and Yanjun, L. (2016). Effects of SDS and SDBS on CO_2 Hydrate Formation, Induction Time, Storage Capacity and Stability at 274.15 K and 5.0 MPa. Chemistry Select 1(19), 6111-6114.

Lin, W.,Delahaye, A., and Fournaison, L. (2008). Phase Equilibrium and Dissociation Enthalpy for Semi-clathrate Hydrate of CO_2 Plus TBAB. Fluid Phase Equilibria 264(1-2), 220-227.

Lirioa, C.F.S. and Pessoab, F.L.P. (2013). Enthalpy of Dissociation of Simple and Mixed Carbon Dioxide Clathrate Hydrate. Chemical Engineering Transactions 32, 577-582.

Ma, Z.W.,Zhang, P.,Bao, H.S., and Deng, S. (2016). Review of Fundamental Properties of CO_2 Hydrates and CO_2 Capture and Separation Using Hydration Method. Renewable and Sustainable Energy Reviews 53, 1273-1302.

Maghsoodloo, B.S. and Abdolmohammad, A. (2015). Effect of Maize Starch on Methane Hydrate Formation/Dissociation Rates and Stability. Journal of Natural Gas Science and Engineering 26, 1-5.

neutrium.net (2015, June 30, 2015). "Hydrate Formation in Gas Systems." Retrieved June 30, 2015.

Prasad, P.S.R. (2014). Methane Hydrate Formation and Dissociation in the Presence of Hollow Silica. Journal of Chemical & Engineering Data 60(2), 304-310.

Roberts, D.W.,Giusti, L., and Forcella, A. (2008). Chemistry of Methyl Ester Sulfonates. Biorenewable Resources 5, 1-8.

Roosta, H.,F., V. and Sh., K. (2014). Experimental Study of CO_2 Hydrate Formation Kinetics with and without Kinetic and Thermodynamic Promoters. Scientia Iranica Transaction Chemistry and Chemical Engineering 21(3), 753-762.

Sabil, K.M.,Witkamp, G.-J., and Peters, C.J. (2010). Estimations of Enthalpies of Dissociation of Simple and Mixed Carbon Dioxide Hydrates from Phase Equilibrium Data. Fluid Phase Equilibria 290(1-2), 109-114.

Saito, Y. (1996). 2nd International Conference on Natural Gas Hydrates, Conference Internationale sur les Hydrates de Gaz Naturel, 1996. Conference on Natural Gas Hydrates. 2, 459–465.

Seo, Y. and Kang, S.-P. (2010). Enhancing CO_2 Separation for Pre-combustion Capture with Hydrate Formation in Silica Gel Pore Structure. Chemical Engineering Journal 161(1-2), 308-312.

Seong-Pil, K. and Jong-Won, L. (2010). Kinetic Behaviors of CO_2 Hydrates in Porous Media and Effect of Kinetic Promoter on The Formation Kinetics. Chemical Engineering Science 65(5), 1840-1845.

Siangsai, A.,Rangsunvigit, P.,Kitiyanan, B.,Kulprathipanja, S., and Linga, P. (2015). Investigation on The Roles of Activated Carbon Particle Sizes on Methane Hydrate Formation and Dissociation. Chemical Engineering Science 126, 383-389.

Sloan, E. and Koh, C.A. (2007). Clathrate Hydrates of Natural Gases Third Edition. Berkeley, California: CRC Press Taylor and Francis Group.

Sun, Q. and Kang, Y.T. (2016). Review on CO_2 Hydrate Formation/Dissociation and Its Cold Energy Application. Renewable & Sustainable Energy Reviews 62, 478-494.

Takeya, S.,Hondoh, A.H.a.T., and Uchida, T. (2000). Freezing-Memory Effect of Water on Nucleation of CO_2 Hydrate Crystals. The Journal of Physical Chemistry B 104, 4164-4168.

Veluswamy, H.P.,Premasinghe, K.P., and Linga, P. (2017). CO_2 Hydrates – Effect of Additives and Operating Conditions on the Morphology and Hydrate Growth. Energy Procedia 105, 5048-5054.

Vysniauskast, A. and Bishnoi, P.R. (1983). A Kinetic Study of Methane Hydrate Formation. Chemical Engineering Science 38, 1061-1197.

Watanabe, K.,Imai, S., and Mori, Y.H. (2005). Surfactant Effects on Hydrate Formation in an Unstirred Gas/Liquid System: An Experimental Study Using HFC-32 and Sodium Dodecyl Sulfate. Chemical Engineering Science 60(17), 4846-4857.

Yang, M.,Liu, W.,Song, Y.,Ruan, X.,Wang, X.,Zhao, J.,Jiang, L., and Li, Q. (2013). Effects of Additive Mixture (THF/SDS) on the Thermodynamic and Kinetic Properties of CO_2/H_2 Hydrate in Porous Media. Industrial & Engineering Chemistry Research 52(13), 4911-4918.

APPENDICES

Appendix A Calculation for the carbon dioxide consumption

From; $$\Delta n_{H\downarrow} = n_{H,t} - n_{H,0} = \left(\frac{PV}{zRT}\right)_{G,0} - \left(\frac{PV}{zRT}\right)_{G,t}$$

where
- $\Delta n_{H\downarrow}$ = moles of consumed gas for hydrate formation (mole)
- $n_{H,t}$ = moles of hydrate at time t, (mole)
- $n_{H,0}$ = moles of hydrate at time 0, (mole)
- P = pressure of the crystallizer, (atm)
- T = temperature of the crystallizer, (K)
- V = the volume of gas phase in the crystallizer, (cm^3)
- z = compressibility factor
- R = the universal gas constant 82.06 cm^3.atm/mol.K

Properties of carbon dioxide

Critical Temperature (T_c)	=	304.2 K
Critical Pressure (P_c)	=	7382 kPa
Acentric Factor (ω)	=	0.228

Properties of additive

Density of sodium dodecyl sulfate (SDS) in pure water	=	1.01 g/cm^3
Molecular weight of SDS	=	288.372 g/mol
Density of methyl ester sulfonate (MES) in pure water	=	g/cm^3
Molecular weight of MES	=	g/mol
Density of tetrahydrofuran (THF) in pure water	=	0.889 g/cm^3
Molecular weight of THF	=	72.11 g/mol

Step 1: To fine pressure reduced (P_r) and temperature reduced (T_r)

Data: Experiment No. 6

At time 0,	Pressure (P)	=	3249.59 kPa	=	32.07 atm
	Temperature (T)	=	276.15 K		
At time t,	Pressure (P)	=	3196.97 kPa	=	31.55 atm
	Temperature (T)	=	276.15 K		

Solution;

$$T_r = \frac{T}{T_c} = \frac{276.15\ K}{304.2\ K} = 0.91$$

$$\text{At time 0, } P_r = \frac{P}{P_c} = \frac{3249.59\ kPa}{7382\ kPa} = 0.44$$

$$\text{At time t, } P_r = \frac{P}{P_c} = \frac{3196.97\ kPa}{7382\ kPa} = 0.43$$

Step 2: To find volume of gas phase (V_{cr}) and volume of additive (V_{add})

Data: Volume of reactor with reservoir ($V_{reactor}$) = 146.94 cm^3

Volume of solution (V_{sol}) = 30.00 cm^3

Volume of gas phase ($V_{reactor} - V_{sol}$) = 146.94 – 30.00 = 116.94 cm^3

Volume of additive (V_{add})

$$V_{add} = \frac{4.5\ mol\ THF}{95.5\ mol\ H_2O} \times \frac{1\ mol\ H_2O}{18\ g\ H_2O} \times \frac{1\ g\ H_2O}{1\ ml\ H_2O} \times \frac{72.11\ g\ THF}{1\ mol\ THF} \times \frac{1\ ml\ THF}{0.889\ g\ THF} \times 100$$

= 21.23 ml in 100 ml H_2O

Therefore, solution 121.23 ml have THF 21.23 ml

$$\text{Solution 30 ml have THF} = \frac{30 \times 21.23}{121.23} = 5.25\ ml$$

$$\text{Solution 30 ml have THF} = 5.25 \text{ ml} \times \frac{0.889 \text{ g}}{1\text{ml}} \times \frac{1 \text{ mol}}{72.11 \text{ g}} = 0.065 \text{ mol}$$

Step 3: To find compressibility factor (z)

$$\beta^0 = \frac{0.083 - 0.422}{T_r^{1.6}} = \frac{0.083 - 0.422}{0.91^{1.6}} = -0.39$$

$$\beta^1 = \frac{0.139 - 0.172}{T_r^{4.2}} = \frac{0.139 - 0.172}{0.91^{4.2}} = -0.049$$

Time 0; $$z = 1 + \beta^0 \frac{P_r}{T_r} + \omega\beta^1 \frac{P_r}{T_r} = 1 + (-0.39)\left(\frac{0.44}{0.91}\right) + (0.228)(-0.049)\left(\frac{0.44}{0.91}\right) = 0.806$$

Time t; $$z = 1 + \beta^0 \frac{P_r}{T_r} + \omega\beta^1 \frac{P_r}{T_r} = 1 + (-0.39)\left(\frac{0.43}{0.91}\right) + (0.228)(-0.049)\left(\frac{0.43}{0.91}\right) = 0.810$$

Step 4: To fine the carbon dioxide consumption

$$\Delta n_{H\downarrow} = \left(\frac{PV}{zRT}\right)_{G,0} - \left(\frac{PV}{zRT}\right)_{G,t}$$

$$= \left(\frac{32.07 \text{ atm} \times 116.94 \text{ cm}^3}{0.806 \times 82.06 \text{ cm}^3\text{atm/mol K} \times 276.15}\right)_{G,0} - \left(\frac{31.55 \text{ atm} \times 116.94 \text{ cm}^3}{0.810 \times 82.06 \text{ cm}^3\text{atm/mol K} \times 276.15}\right)_{G,t}$$

$$= 0.2053 - 0.2010 = 0.0043 \text{ mol}$$

Therefore, the carbon dioxide consumption is 0.0043 mol

$$\text{Carbon dioxide consumption} = \frac{0.0043 \text{ mol } CO_2}{21.24 \text{ ml } H_2O} \times \frac{18 \text{ ml } H_2O}{1 \text{ mol } H_2O} = 0.00364 \text{ mol } CO_2/\text{mol } H_2O$$

Appendix B Calculation for the percentage of carbon dioxide recovery

Data: Experiment No. 6

$$\text{From;} \qquad \%\ \text{carbon dioxide recovery} = \frac{\Delta n_{H\uparrow}}{\Delta n_{H\downarrow}} \times 100 \qquad (3.4)$$

where $\Delta n_{H\uparrow}$ = moles of consumed gas for hydrate dissociation, (mole)

$\Delta n_{H\downarrow}$ = moles of consumed gas for hydrate formation, (mole)

$$\text{Thus,} \quad \%\ \text{carbon dioxide recovery} = \frac{0.005760515}{0.031918919} \times 100 = 18.05\%$$

CURRICULUM VITAE

Name: Ms. Thiphakorn Absuwan

Date of Birth: January 12, 1995

Nationality: Thai

University Education:

2013–2017 Bachelor Degree of Petrochemical and Polymeric Materials Engineering, Faculty of Engineering and Industrial Technology, Silpakorn University, Nakhon Pathom, Thailand.

Work Experience:

May – June 2015	Position:	Internship Student
	Company name:	PTT Global Chemical

Proceeding:

1. Absuwan, T., Kulprathipanja, S., and Rangsunvigit, P. (2019, May 30) Green-house Gas Storage through Enhanced Hydrate Formation – Effects of Promoters on Gas Uptake and Induction Time. Proceedings of the The 25th PPC Symposium on Petroleum, Petrochemicals, and Polymers and The 10th Research Symposium on Petrochemical and Materials Technology" (PPC & PETROMAT Symposium 2019), Chulalongkorn University, Thailand.

Presentations:

1. Absuwan, T., Udomkitpanya, T., Jariyama, S., and Udomkitpanya, P. (2017, May 31 – June 2) Effect of Zeolite on Thermal Properties and Rheological Properties of PET/PBAT Blend Film. Poster presented at The 3rd International Conference on Applied Physics and Material Applications 2017, Pattaya, Thailand.
2. Absuwan, T., Kulprathipanja, S., and Rangsunvigit, P. (2018, November 8-9) Green-house Gas Storage Through Enhanced Hydrate Formation. Poster presented at Thai Institute of Chemical Engineering and Applied Chemistry (TIChE) Conferences 2018, Pattaya, Thailand.